Topological Materials Predicted by OpenMX

Hongming Weng (翁红明)

Institute of Physics,
Chinese Academy of Sciences

Nov. 23-25@KAIST, Daejeon

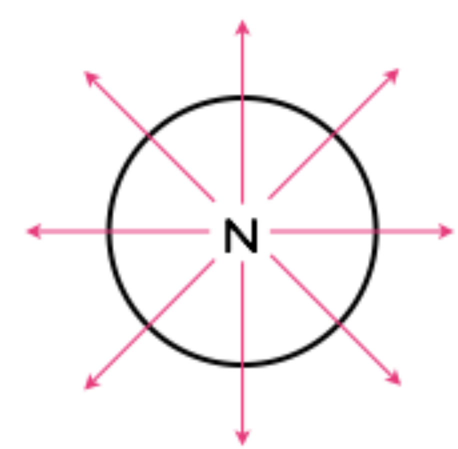

2016 Nobel Prize in Physics

David J. Thouless
University of Washington, Seattle, WA, USA

F. Duncan M. Haldane
Princeton University, NJ, USA

J. Michael Kosterlitz
Brown University, Providence, RI, USA

"for theoretical discoveries of topological phase transitions and topological phases of matter"

They revealed the secrets of exotic matter

TKNN number

Quantized Hall Conductance in a Two-Dimensional Periodic Potential

D. J. Thouless, M. Kohmoto,[a] M. P. Nightingale, and M. den Nijs
Department of Physics, University of Washington, Seattle, Washington 98195
(Received 30 April 1982)

The Hall conductance of a two-dimensional electron gas has been studied in a uniform magnetic field and a periodic substrate potential U. The Kubo formula is written in a form that makes apparent the quantization when the Fermi energy lies in a gap. Explicit expressions have been obtained for the Hall conductance for both large and small $U/\hbar\omega$.

Because of the relation between the velocity operator and the derivatives of $\hat{H}$, the Kubo formula can be written as

$$\sigma_{\rm H} = \frac{ie^2}{A_0\hbar} \sum_{\epsilon_\alpha < E_{\rm F}} \sum_{\epsilon_\beta > E_{\rm F}} \frac{(\partial \hat{H}/\partial k_1)_{\alpha\beta}(\partial \hat{H}/\partial k_2)_{\beta\alpha} - (\partial \hat{H}/\partial k_2)_{\alpha\beta}(\partial \hat{H}/\partial k_1)_{\beta\alpha}}{(\epsilon_\alpha - \epsilon_\beta)^2}, \qquad (4)$$

where A_0 is the area of the system and $\epsilon_\alpha, \epsilon_\beta$ are eigenvalues of the Hamiltonian. This can be related to the partial derivatives of the wave functions u, and gives

$$\sigma_{\rm H} = \frac{ie^2}{2\pi h} \sum \int d^2k \int d^2r \left(\frac{\partial u^*}{\partial k_1}\frac{\partial u}{\partial k_2} - \frac{\partial u^*}{\partial k_2}\frac{\partial u}{\partial k_1} \right)$$
$$= \frac{ie^2}{4\pi h} \sum \oint dk_j \int d^2r \left(u^* \frac{\partial u}{\partial k_j} - \frac{\partial u^*}{\partial k_j} u \right), \qquad (5)$$

where the sum is over the occupied electron subbands and the integrations are over the unit cells in r and k space. The integral over the k-space unit cell has been converted to an integral around the unit cell by Stokes's theorem. For nonoverlapping subbands ψ is a single-valued analytic function everywhere in the unit cell, which can only change by an r-independent phase factor θ when k_1 is changed by $2\pi/aq$ or k_2 by $2\pi/b$. The integrand reduces to $\partial\theta/\partial k_j$. The integral is $2i$ times the change in phase around the unit cell and must be an integer multiple of $4\pi i$.

The problem of evaluating this quantum number remains. We have considered the potential

$$U(x,y) = U_1 \cos(2\pi x/a) + U_2 \cos(2\pi y/b), \qquad (6)$$

both in the limit of a weak periodic potential ($|U| \ll \hbar\omega_c$) and in the tight-binding limit of a strong periodic potential. In the weak-potential limit the wave function can be written as a superposition of the nearly degenerate Landau functions in

Haldane Model

VOLUME 61, NUMBER 18 PHYSICAL REVIEW LETTERS 31 OCTOBER 1988

Model for a Quantum Hall Effect without Landau Levels: Condensed-Matter Realization of the "Parity Anomaly"

F. D. M. Haldane
Department of Physics, University of California, San Diego, La Jolla, California 92093
(Received 16 September 1987)

A two-dimensional condensed-matter lattice model is presented which exhibits a nonzero quantization of the Hall conductance σ^{xy} in the *absence* of an external magnetic field. Massless fermions *without spectral doubling* occur at critical values of the model parameters, and exhibit the so-called "parity anomaly" of (2+1)-dimensional field theories.

PACS numbers: 05.30.Fk, 11.30.Rd

$$\mathbf{H}(\mathbf{k}) = 2t_2\cos\phi\left(\textstyle\sum_i \cos(\mathbf{k}\cdot\mathbf{b}_i)\right)\mathbf{I} + t_1\left(\textstyle\sum_i [\cos(\mathbf{k}\cdot\mathbf{a}_i)\sigma^1 + \sin(\mathbf{k}\cdot\mathbf{a}_i)\sigma^2]\right) + \left[M - 2t_2\sin\phi\left(\textstyle\sum_i \sin(\mathbf{k}\cdot\mathbf{b}_i)\right)\right]\sigma^3, \quad (1)$$

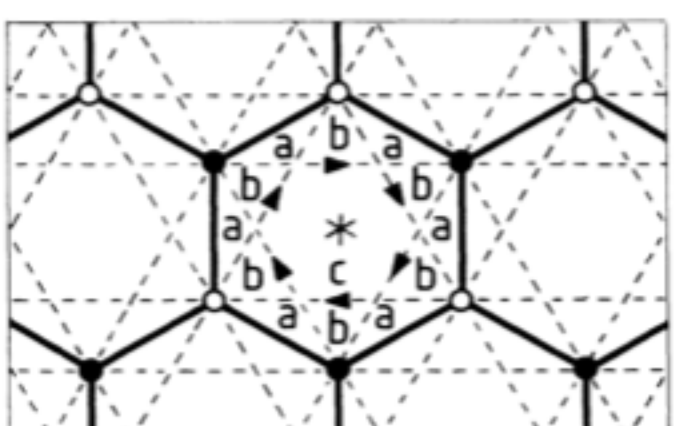

a

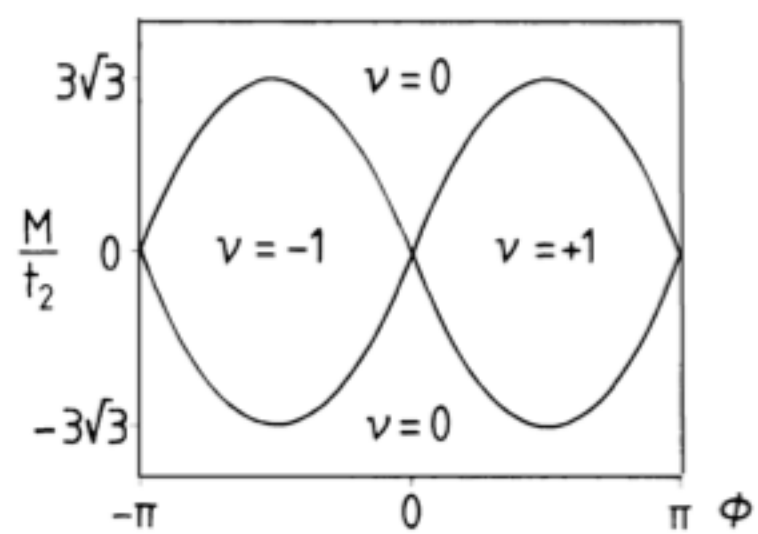

Outline

- Band topology theory

  Topological insulator (TI) and

  Topological Semimetal (TS): the topological metal in 3D

TS family

- Dirac semi-metal (DSM)
- Weyl semi-metal (WSM)
- Node-line semi-metal (NLSM)
- Triply-degenerate Nodal Point semi-metal (TDNP)

Review papers on topological quantum states from first-principles calculations

Hongming Weng, Xi Dai and Zhong Fang, *MRS Bulletin* **39**, 849 (2014)

Hongming Weng, Rui Yu, Xiao Hu, Xi Dai and Zhong Fang, *Adv. Phys.* **64**, 227 (2015)

Hongming Weng, Xi Dai and Zhong Fang, J. Phys.: Condens. Matter **28**, 303001 (2016)

Insulator & Metal from Band Theory

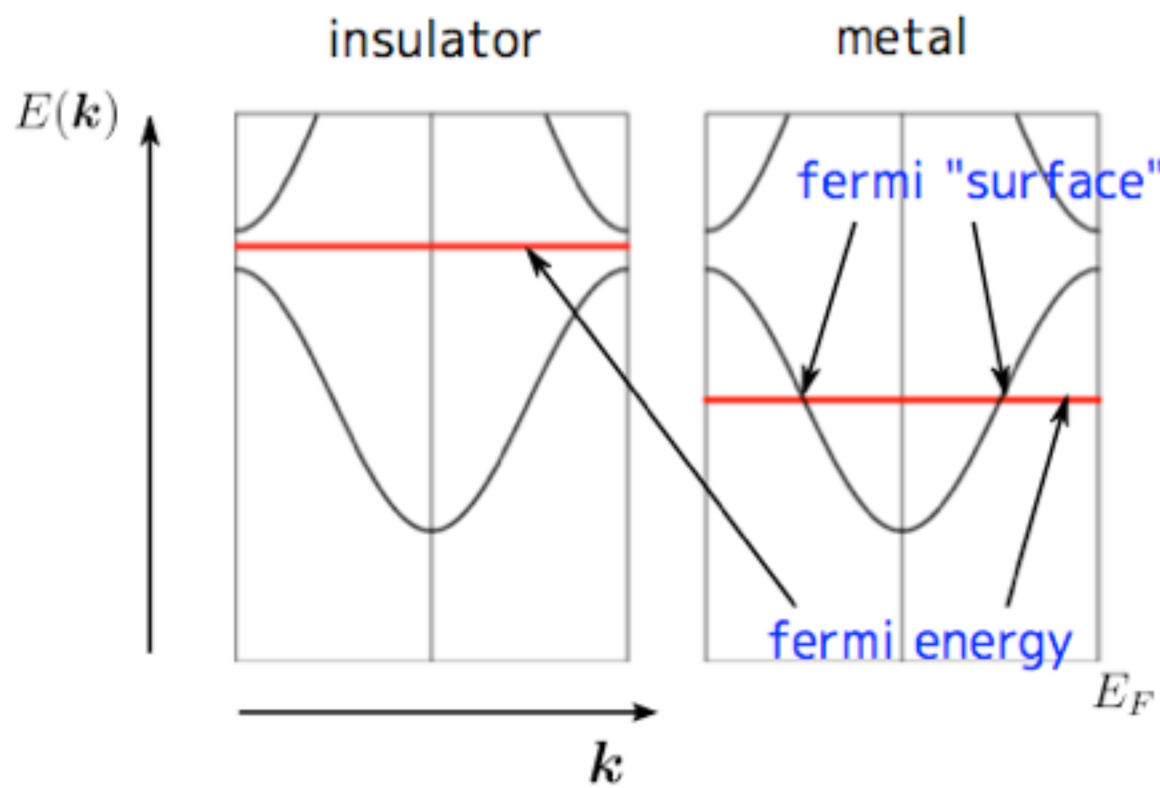

crystal momentum in
1st Brillouin Zone, BZ

cell-periodic hamiltonian

$$\hat{H}(\vec{k}) = e^{-i\vec{k}\cdot\vec{r}}\hat{H}e^{i\vec{k}\cdot\vec{r}}$$

$$u_{n,\vec{k}}(\vec{r}) = e^{-i\vec{k}\cdot\vec{r}}\psi_{n,\vec{k}}(\vec{r})$$

$$\hat{H}(\vec{k})|u_{n,\vec{k}}(\vec{r})\rangle = E_n(\vec{k})|u_{n,\vec{k}}(\vec{r})\rangle$$

What are hidden/ignored?

Quantum geometrical phase revealed by M.V. Berry.

Introduction to Berry Phase

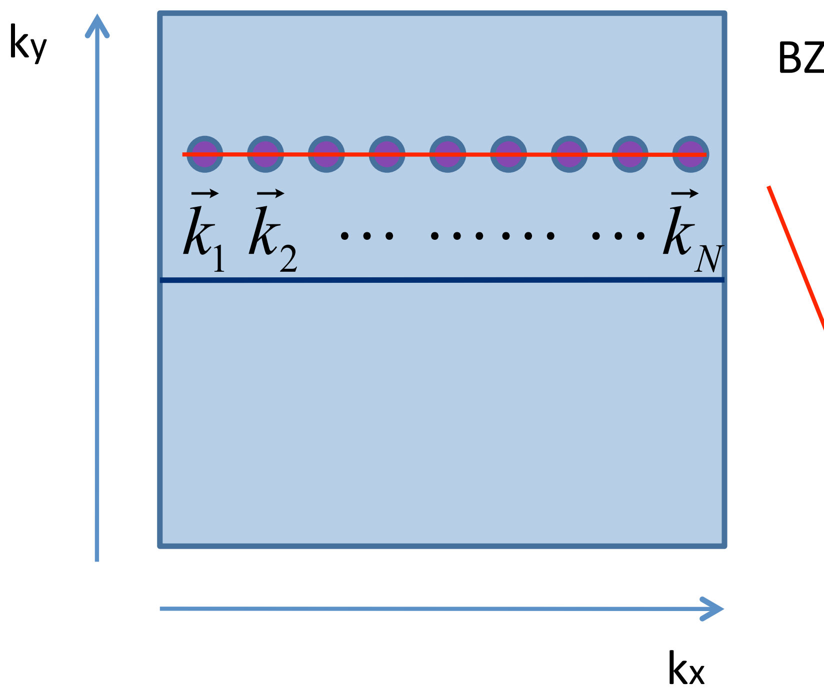

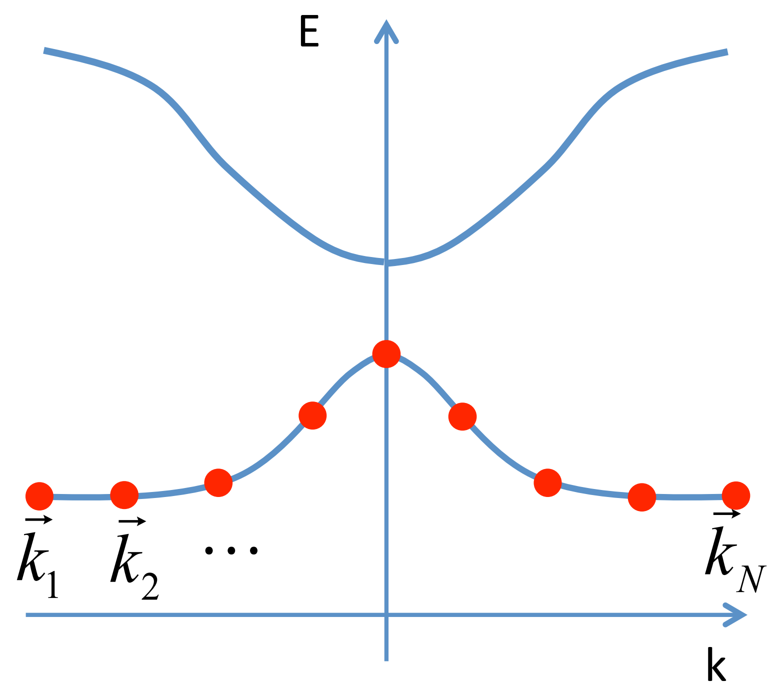

Wilson loop method

$$\langle u_{\vec{k}_1}|u_{\vec{k}_2}\rangle\langle u_{\vec{k}_2}|u_{\vec{k}_3}\rangle\cdots\cdots\boxed{\langle u_{\vec{k}_{N-1}}|u_{\vec{k}_N}\rangle}\langle u_{\vec{k}_N}|u_{\vec{k}_1}\rangle = Ae^{i\theta(k_y)}$$

Berry connection

Meaning of the phase：
the center of the Wannier
function for 1D band insulator
or the charge center

A. Soluyanov, D. Vanderbilt, Phys. Rev. B **83**, 235401 (2011)
Yu, R., Qi, X. L., Bernevig, B., Fang, Z. & Dai, X. Phys. Rev. B **84**, 075119 (2011).

Berry Phase & Band Topology

$\theta_n(k_y)$ is the center position of the n'th Wannier function.

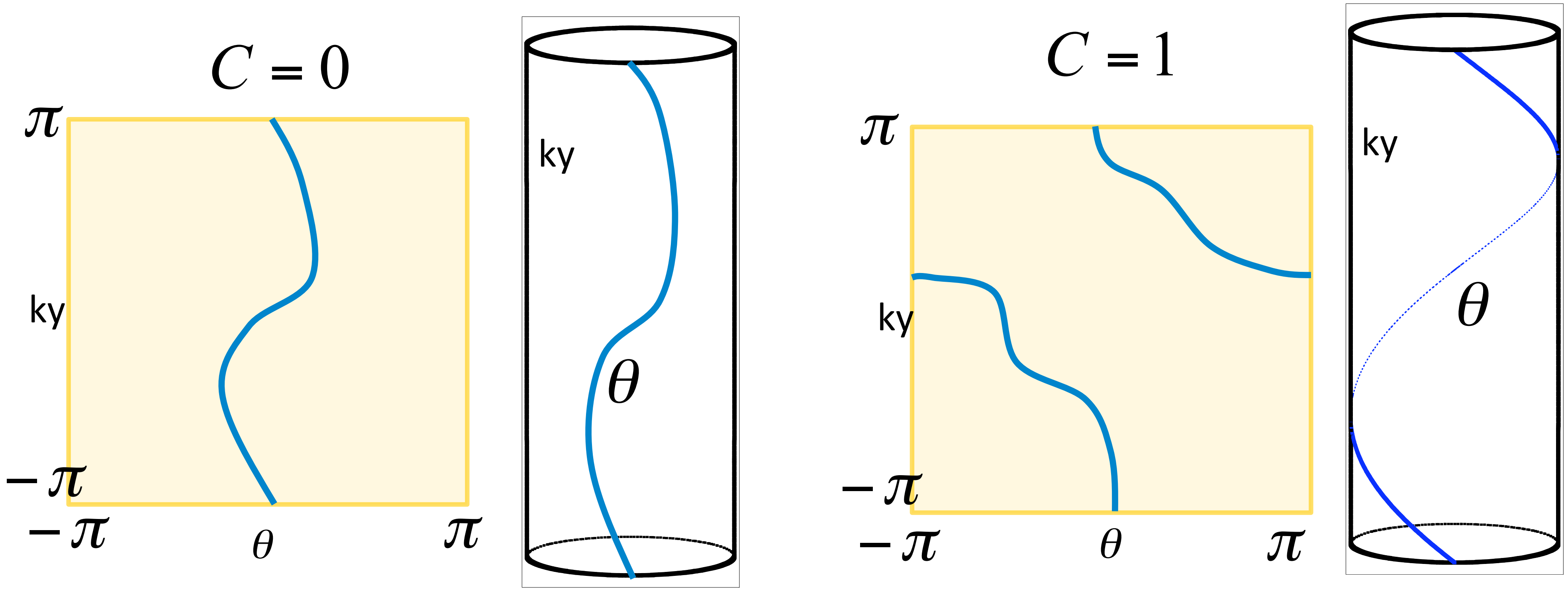

A. Soluyanov, D. Vanderbilt, Phys. Rev. B **83**, 235401 (2011)
Yu, R., Qi, X. L., Bernevig, B., Fang, Z. & Dai, X. Phys. Rev. B **84**, 075119 (2011).

Hongming Weng, R. Yu, X. Hu, X. Dai, Z. Fang, Adv. Phys. **64**, 227 (2015)

Berry Phase & Band Topology

time-reversal symmetry makes $\theta(k_y)$ is doubly degenerate at ky=0 and ky= π

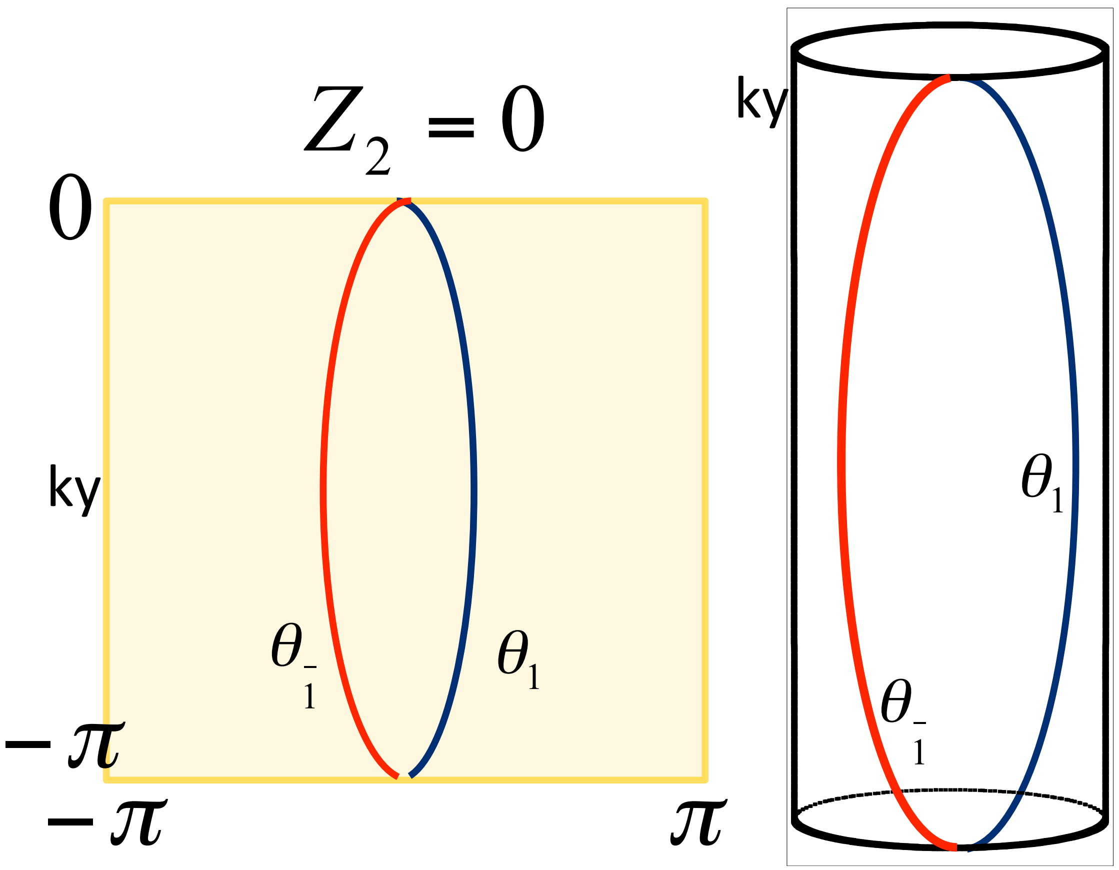

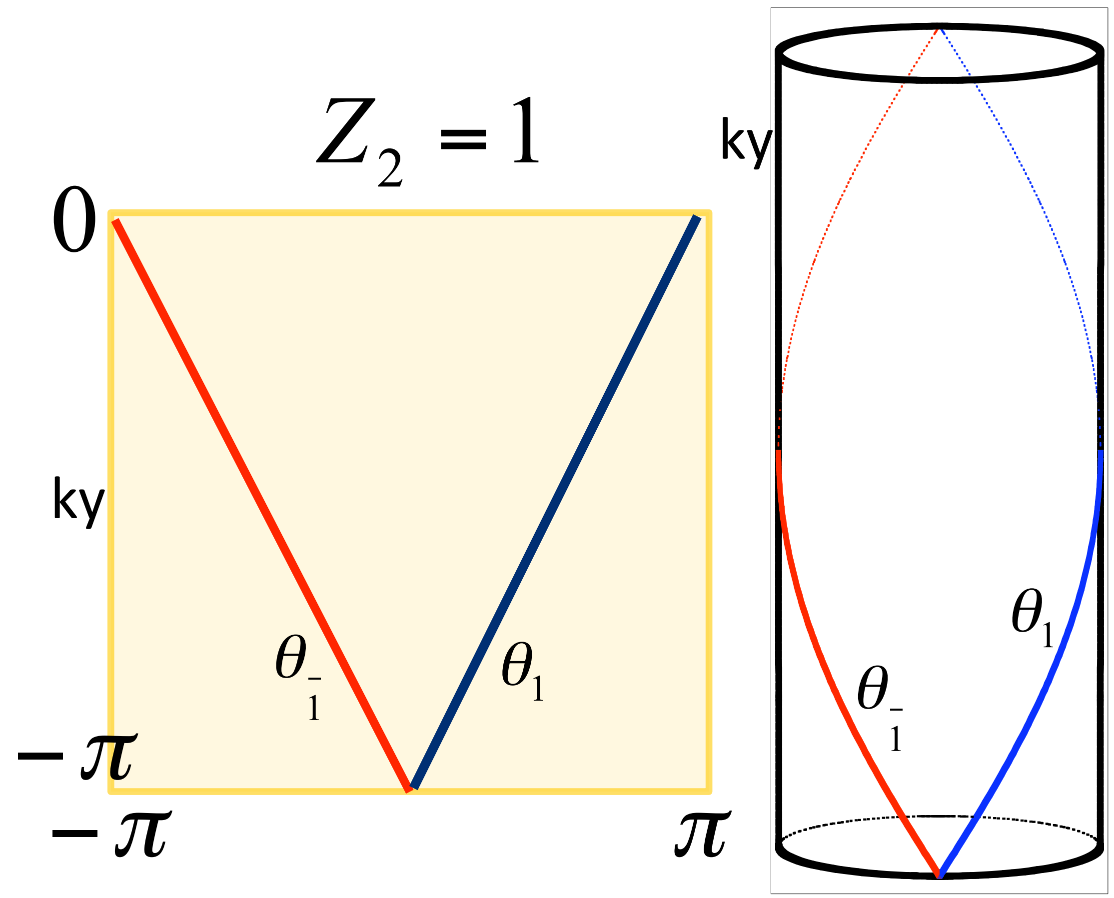

A. Soluyanov, D. Vanderbilt, Phys. Rev. B **83**, 235401 (2011)
Yu, R., Qi, X. L., Bernevig, B., Fang, Z. & Dai, X. Phys. Rev. B **84**, 075119 (2011).

Hongming Weng, R. Yu, X. Hu, X. Dai, Z. Fang, Adv. Phys. **64**, 227 (2015)

Magnetic Monopole & Band topology

$$\psi_{n\mathbf{k}}(\mathbf{r}) = e^{i\mathbf{k}\cdot\mathbf{r}} u_{n\mathbf{k}}(\mathbf{r}) e^{i\phi_n(\mathbf{k})}$$

$$\phi_n = \oint_C \vec{A}(\vec{k})d\vec{k}$$

$$= \iint_{S(c)} \Omega_z(\vec{k})dk^2$$

$$\vec{A}(\vec{k}) = \sum_n < n\vec{k}|\vec{\nabla}_k|n\vec{k} >$$

$$\vec{\Omega}(\vec{k}) = \vec{\nabla}_k \times \vec{A}(\vec{k})$$

2D BZ

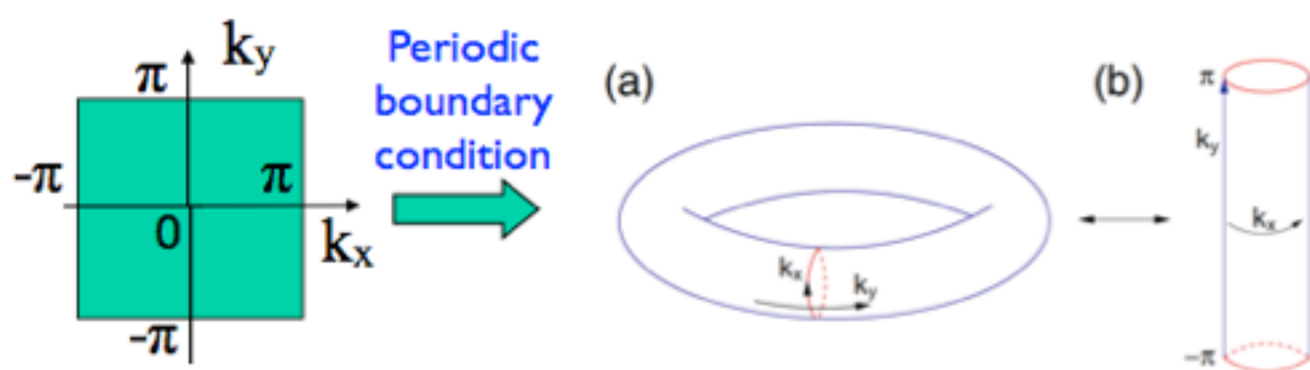

Gauss' theorem

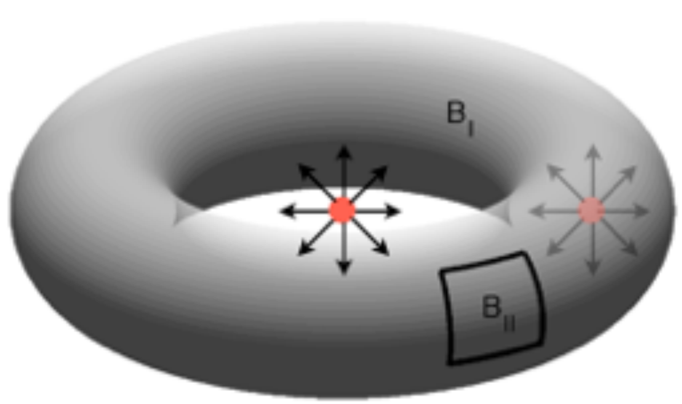

number of monopole enclosed
by momentum space

$\phi_n(\mathbf{k})$ winding number

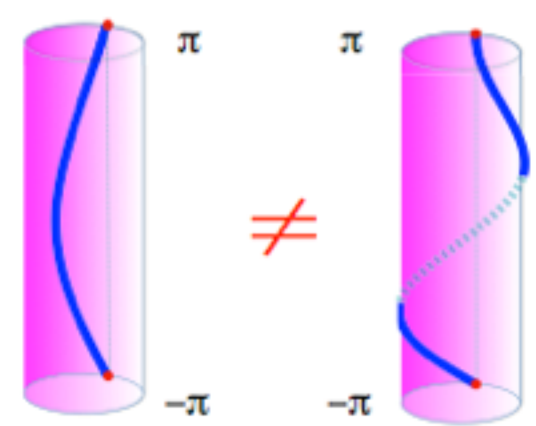

winding number

Magnetic Monopole & Band topology

Insulator vs. Metal

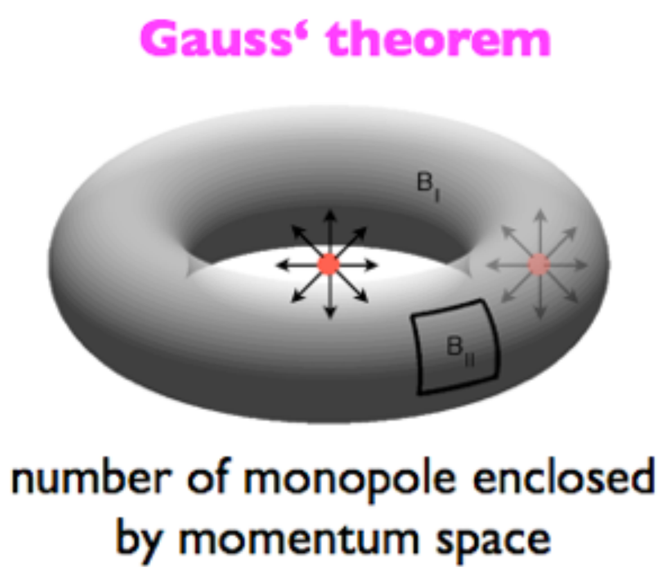

The adiabatic loop does not necessarily passing through the magnetic monopole.

$$\frac{1}{2\pi}\oint_{FS}\vec{\Omega}(k)\cdot dS(k) = C_{FS}$$

Defined on 2D Fermi surface
of a 3D metallic system

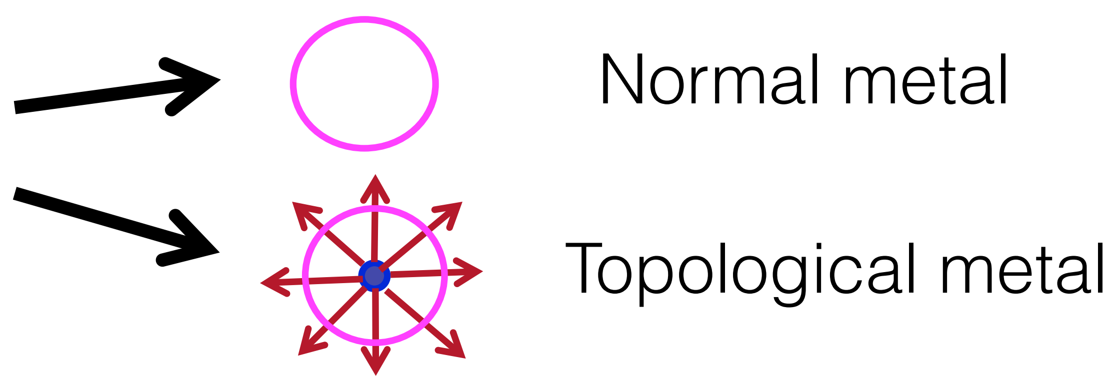

Generalized from whole Brillouin zone in *insulators* to
any closed manifold in crystal momentum space.

Z. Wang, Y. Sun, X. Chen, C. Franchini, G. Xu, H. Weng*, Z. Fang+ and X. Dai, Phys. Rev. B **85**, 195320 (2012)
H. Weng, R. Yu, X. Hu, X. Dai, Z. Fang, Adv. Phys. **64**, 227(2015)

State of matter from Band Topology

Insulator:
no fermi surface

?Metal?
Three types of Fermi surface

Insulators

No fermi surface

Normal Insulator
+
Topologically nontrivial Insulator

Metals

Semi-metal (Dirac, Weyl)

Nodal line

Fermi surface

Femi points (in bulk)
Fermi arcs (on surface)

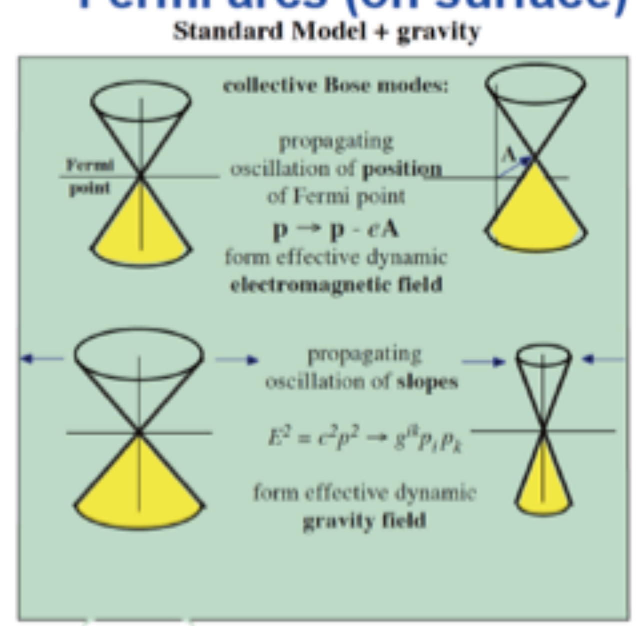

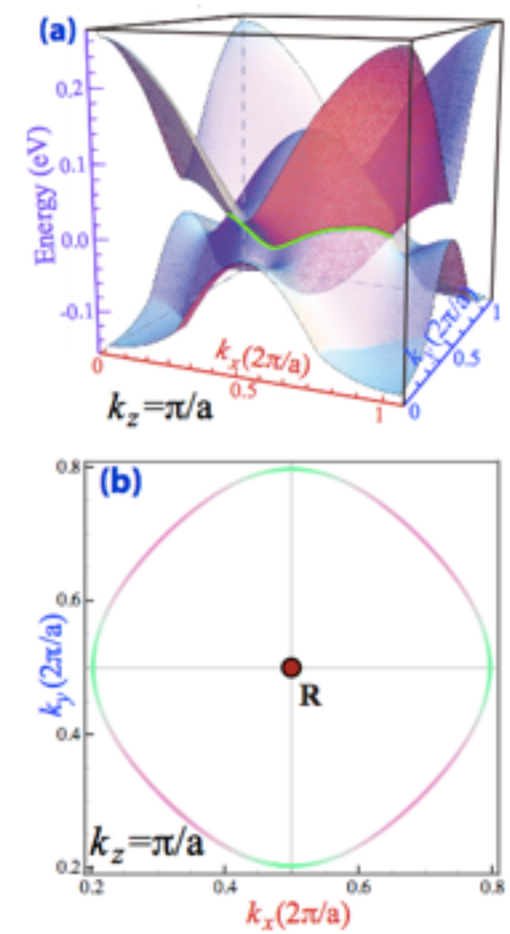

Normal Metal + Topological Semi-metal

Extended the concept of topology to metal.
- Weyl Semimetal
- Dirac Semimetal
- Node-line Semimetal

Recent Research Interests

1. Explore new Topological Quantum States

Dirac Semimetal: Na_3Bi (PRB'12, Science'14) Cd_3As_2 (PRB'13, Nat.Mater.'14)

Weyl Semimetal: $HgCr_2Se_4$ (PRL'11), TaAs (3xPRX'15, Nat. Phys.'15, PRL'15, Nat. Commun.'16)

Node-line Semimetal: 3D carbon crystal (PRB'15, PRL'16), Cu_3PdN(PRL'15)

Triply-Degenerated-Nodal-Point semimetal: TaN (PRB'16), ZrTe (PRB'16)

2. Understand new Topological Quantum Phenomena

Correlated Topological Insulator

SmB_6 (PRL'12, Nat. Commun.'14)

YbB_6 & YbB_{12} (PRL'14)

3. Predict new Topological Materials

Ag_2Te (PRL'11) Strongly anisotropic surface Dirac cone

$ZrTe_5$&$HfTe_5$ (PRX'14,PRX'16), MXene (PRB'15), ZrSiO (PRB'15) Large band-gap 2D TI

TlN(PRB'14) "negative" spin-orbit coupling TI

Highly Efficient computational tools is the basis

1, Local orbital base and pseudo-potential methods

2, Wannier function analysis

3, LDA++ methods: +Gutzwiller, +DMFT etc.

4, Material database

Methodology

I, Local orbital base and pseudo-potential methods

Advantage：

+ Quickly obtain electronic structure
+ from $O(N^3)$ to $O(N)$
+ spin-orbit coupling
+ structural optimization & molecular dynamic
+ non-collinear magnetism
+ structural code & easy to be extended

Disadvantage:

+ cut-off appro. & basis completeness
+ pseudo-potential

http://www.openmx-square.org

Methodology

2, Wannier function analysis

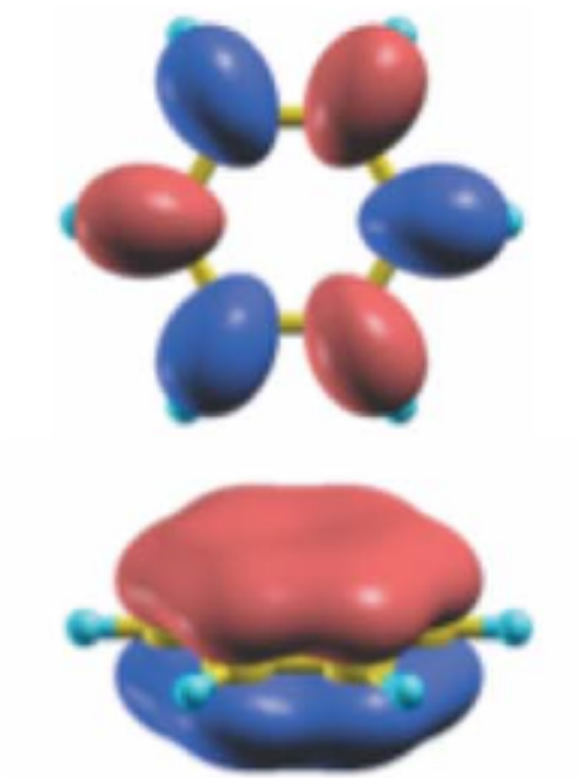

Advantage：

+ Intuitive picture；
+ accurate minimal basis；
+ highly efficient integration

Features of our code：

+ flexible projector；
+ symmetrized。

Hongming Weng,* T. Ozaki, and K. Terakura, Phys. Rev. B **79**, 235118 (2009)

Recent developments:

1. Boundary state calculation: slab model & Green's function method
2. Spin texture
3. Wilson loop calculation
4. Parity calculation
5. Anomalous Hall Conductivity calcualtion

Dirac & Weyl Fermion

Dirac Fermion (1928) 4x4

$$\begin{pmatrix} \hat{E} - c\boldsymbol{\sigma}\cdot\hat{\mathbf{p}} & 0 \\ 0 & \hat{E} + c\boldsymbol{\sigma}\cdot\hat{\mathbf{p}} \end{pmatrix}\psi = mc^2\begin{pmatrix} 0 & I_2 \\ I_2 & 0 \end{pmatrix}\psi$$

$$E(k) = \pm\sqrt{k^2 + m^2}$$

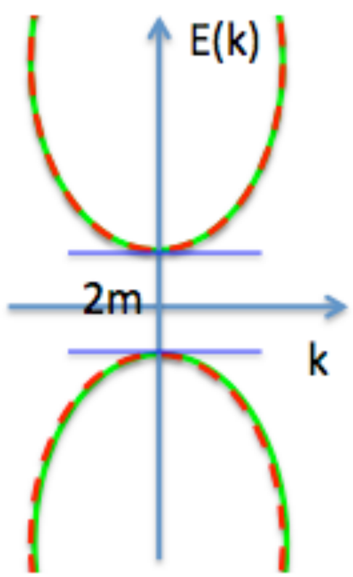

Massive Dirac Fermion

Massless Dirac Fermion (1929)

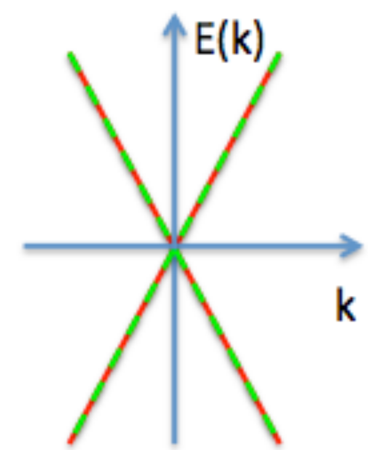

Massless Dirac Fermion

Weyl fermion 2x2

$$H(\vec{k}) = \vec{k}\cdot\vec{\sigma} = \begin{bmatrix} k_z & k_x - ik_y \\ k_x + ik_y & -k_z \end{bmatrix}$$

Massless Dirac Fermion: two Weyl Fermions with opposite topological charges "kiss".

L. Balents, Weyl electrons kiss. Physics **4**, 36 (2011).

X. Wan *et al.* Phys.Rev.B **83**, 205101 (2011).

Dirac & Weyl Semimetal

Transition state between TI and NI in 3D

S. Murakami et al. arXiv:1006.1188
Physica E **43**, 748–754 (2011)

no Inversion symmetry

with Inversion symmetry

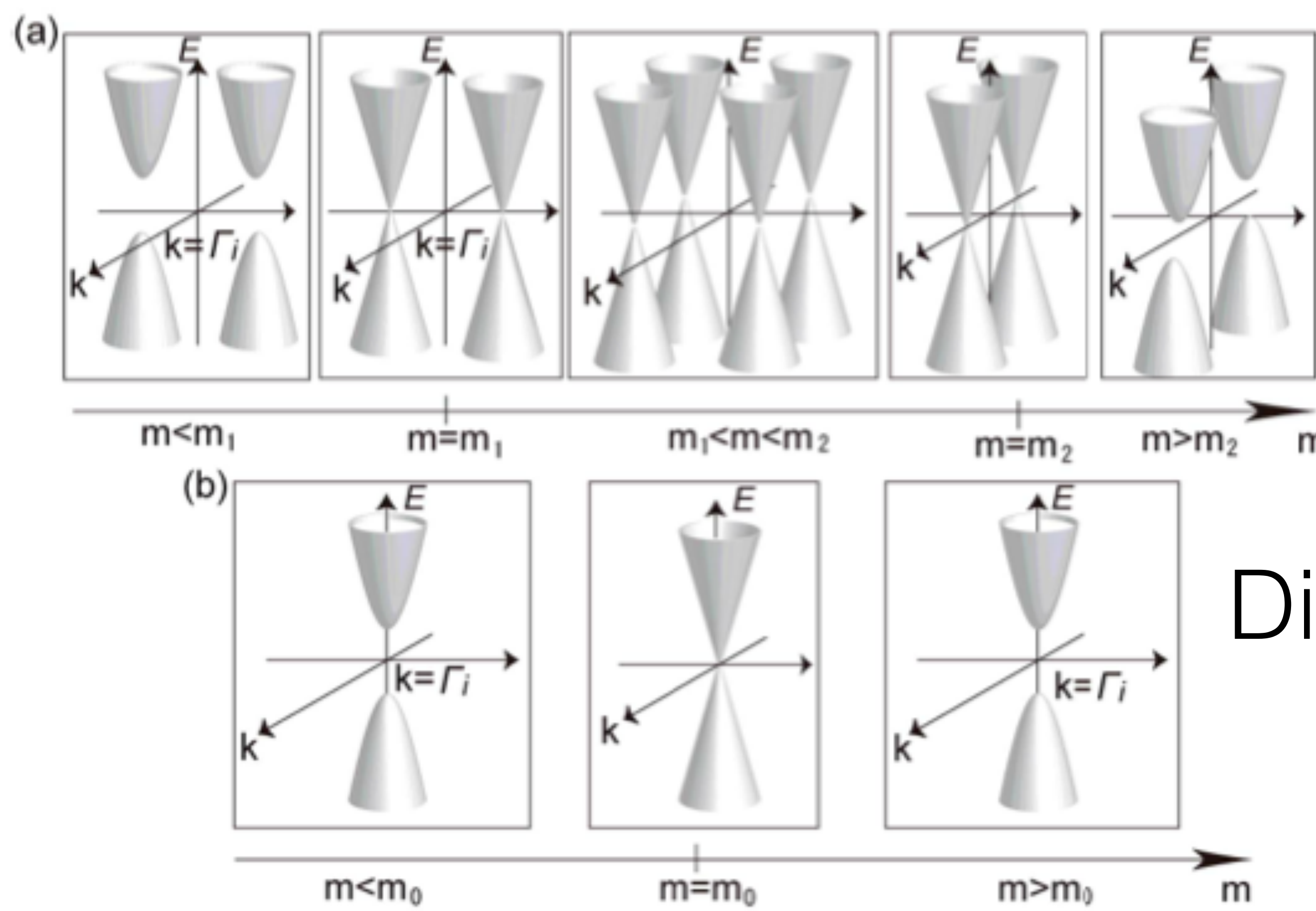

Weyl nodes

Dirac nodes

Fragile and hard to control.

3D metal with low energy exaction behaving the same as massless Dirac/Weyl fermion.

Dirac Semimetal with Band Inversion

as “singularity point” of various topological states

mass term

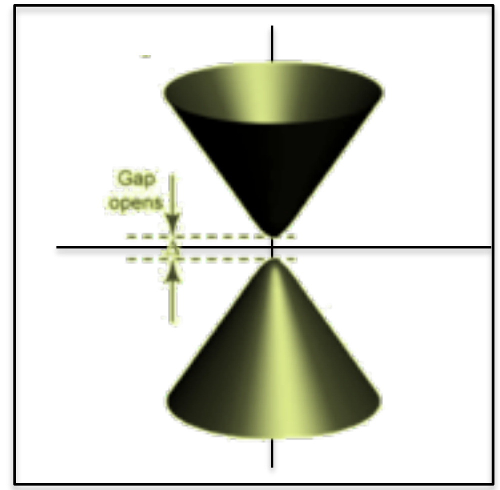

Normal
OR
Topological
Insulator

“3d graphene"

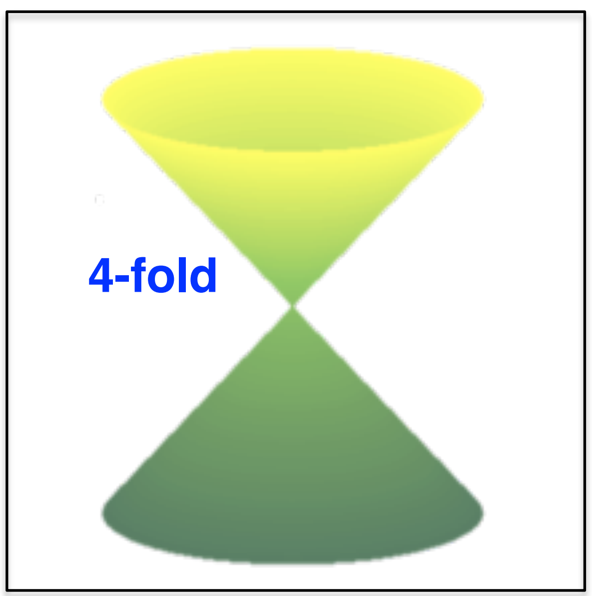

Na_3Bi & Cd_3As_2

The only two DSMs widely studied experimentally.

breaking Inversion symmetry

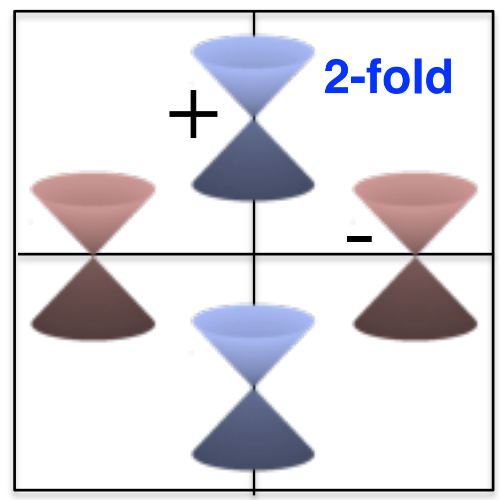

Noncentrosymmetric
& nonmagnetic Weyl
Semimetal

TaAs-family(PRX’15)

breaking Time reversal symmetry

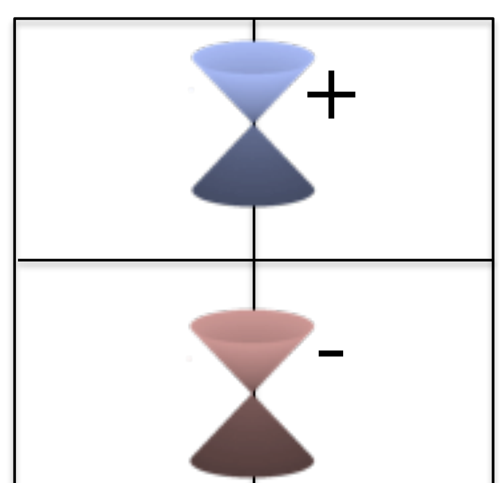

Magnetic Weyl
Semimetal

$A_2Ir_2O_7$ (X. Wan et al PRB’11),
$HgCr_2Se_4$ (PRL’11)

Fermi arcs of WSM

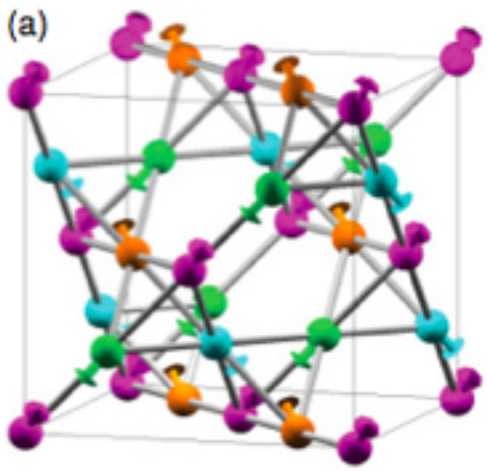

$Y_2Ir_2O_7$

Fermi arcs on the surface

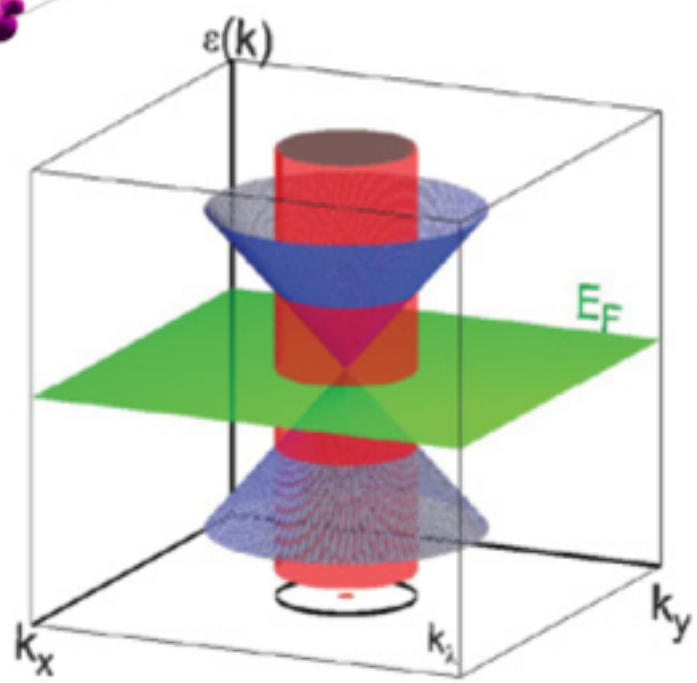

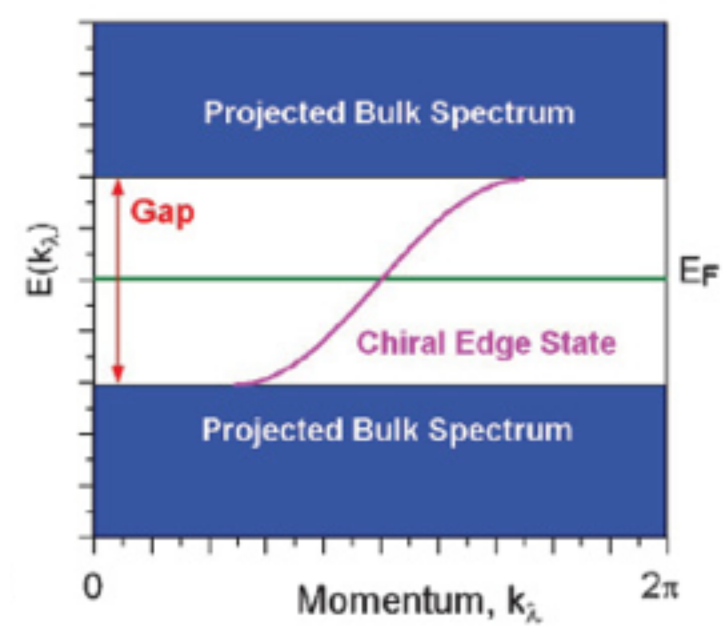

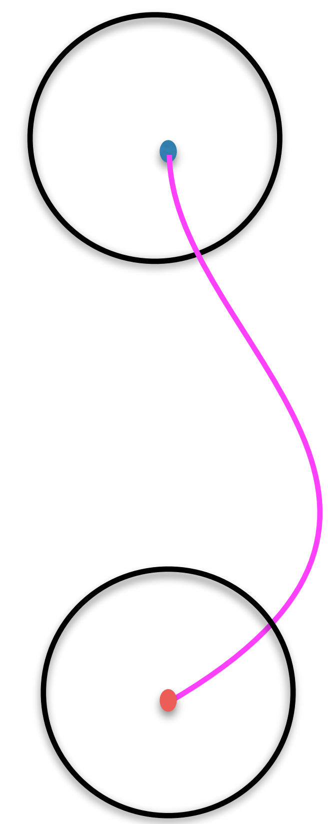

Topview

Xiangang Wan *et al.* Phys.Rev.B **83**,205101 (2011)

Crystal structure of TaAs family

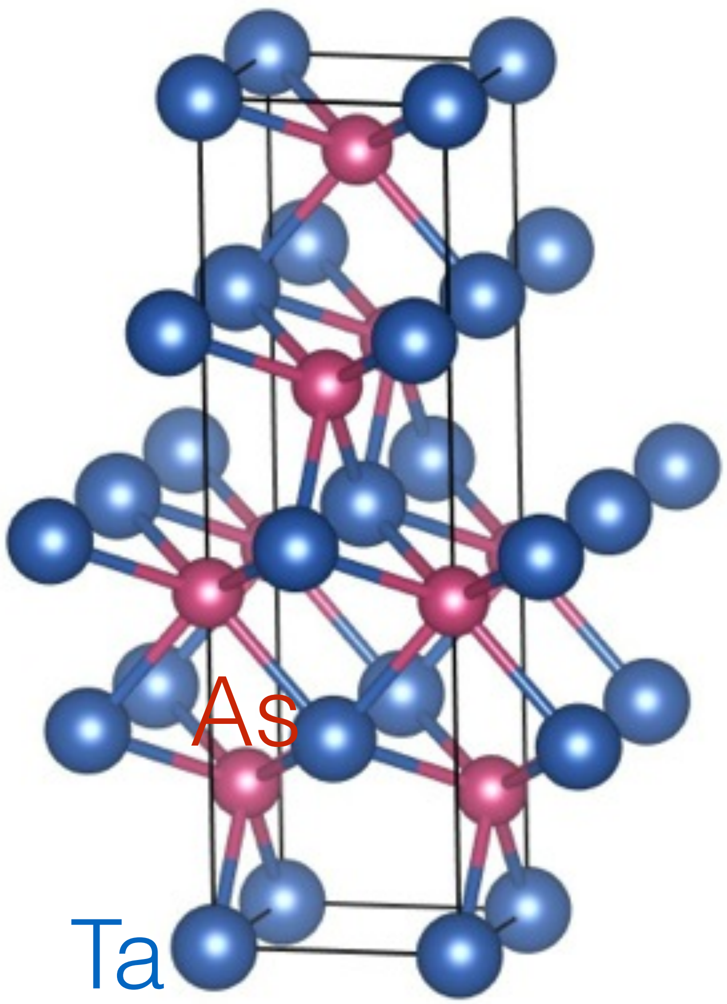

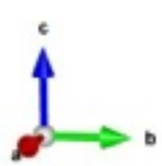

Space group $I4_1md$ (No. 109)
Body-centered tetragonal (BCT) structure

Both Ta and As are at *4a* Wyckoff position.
$(0,0,u)$ and $u_{Ta}=0.0$.

	a=b	c	*u*
TaAs	3.4348	11.641	0.417
TaP	3.3184	11.363	0.416
NbAs	3.4517	11.680	0.416
NbP	3.33242	11.37059	0.417

S. Furuseth, K. Selte and A. Kjekshus,
Acta Chem. Scand. **19**, 95 (1965)

Hongming Weng*, Chen Fang, Zhong Fang, A. Bernevig, Xi Dai,
http://arxiv.org/abs/1501.00060 posted on Dec. 31, 2014 and
Published as Phys. Rev. X 5, 011029 (2015) in March, 2015.

a similar work from Princeton group
http://arxiv.org/abs/1501.00755 posted on Jan. 5, 2015 and
published as Nat. Commun. 6, 7373 (2015) in Jun. 2015

Known properties of TaAs family

NbAs

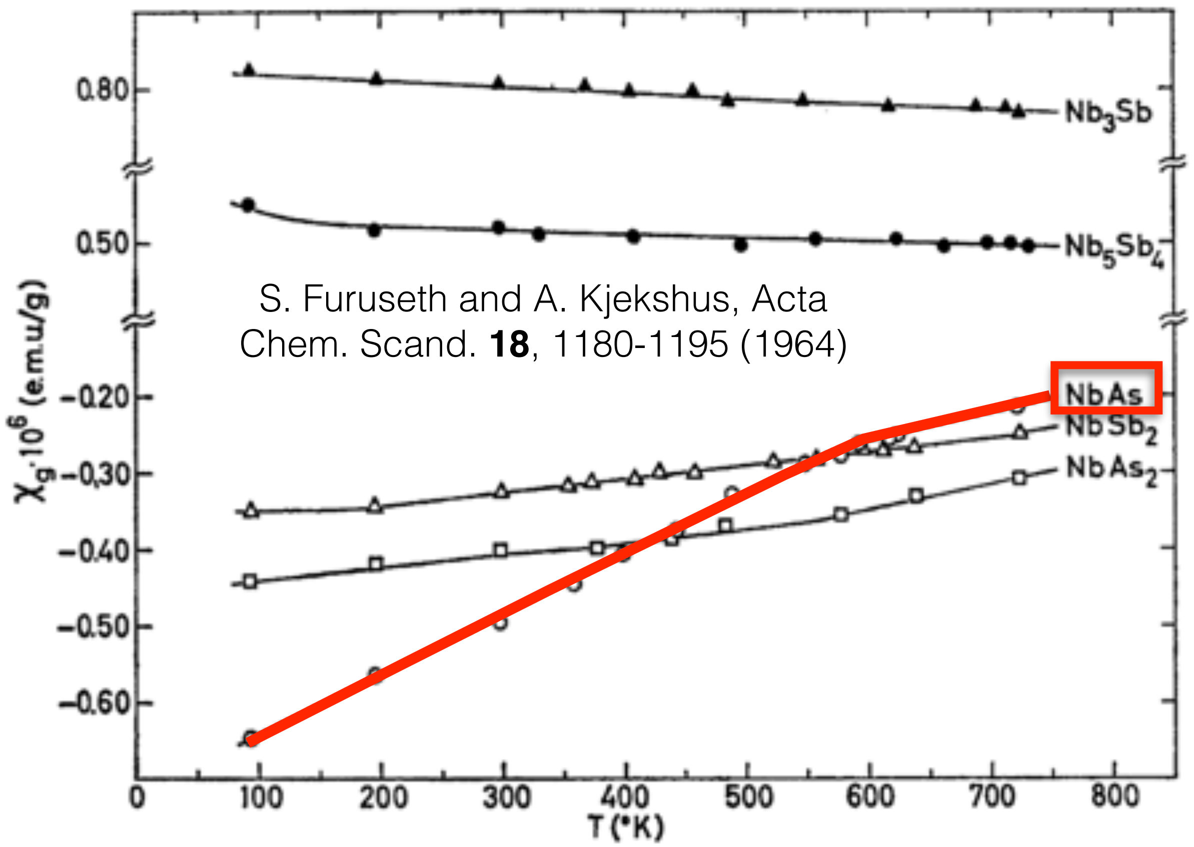

Fig. 5. The magnetic susceptibilities of NbAs, $NbAs_2$, Nb_3Sb, Nb_5Sb_4, and $NbSb_2$ as a function of temperature.

TaAs

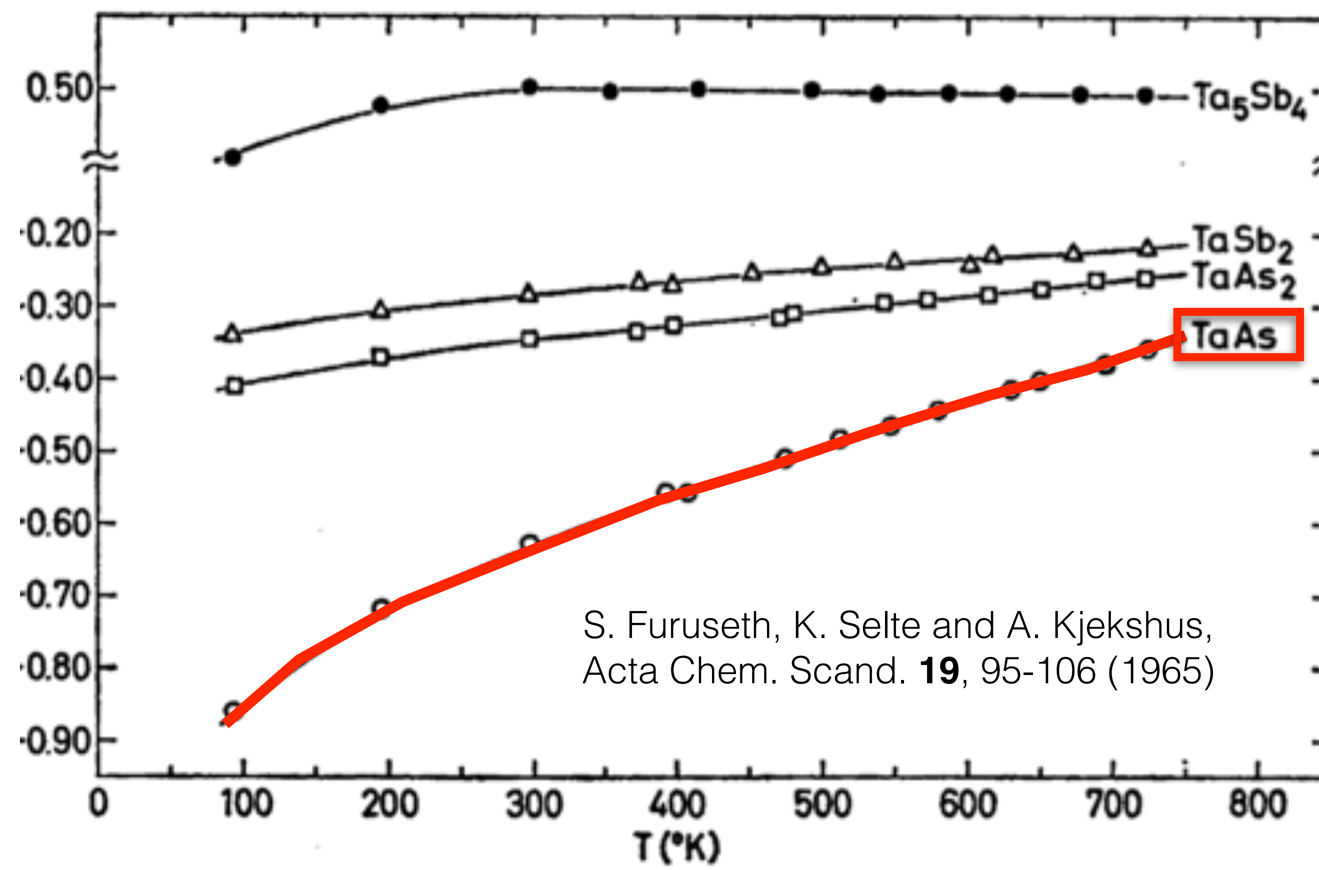

TABLE V. Magnetic susceptibilities of NbP and TaP.

Compound	T(°K)	X_g(10^{-6} cgs/g)
NbP	78	−0.45±0.03
	201	−0.57±0.03
	297	−0.52±0.02
	373	−0.55±0.03
TaP	78	−0.70±0.03
	201	−0.65±0.03
	297	−0.62±0.02
	373	−0.59±0.02

B. A. Scott,G. R. Eulenberger, and R. A. Bernheim, J. Chem. Phys. **48**, 263 (1968)

Band structure of TaAs

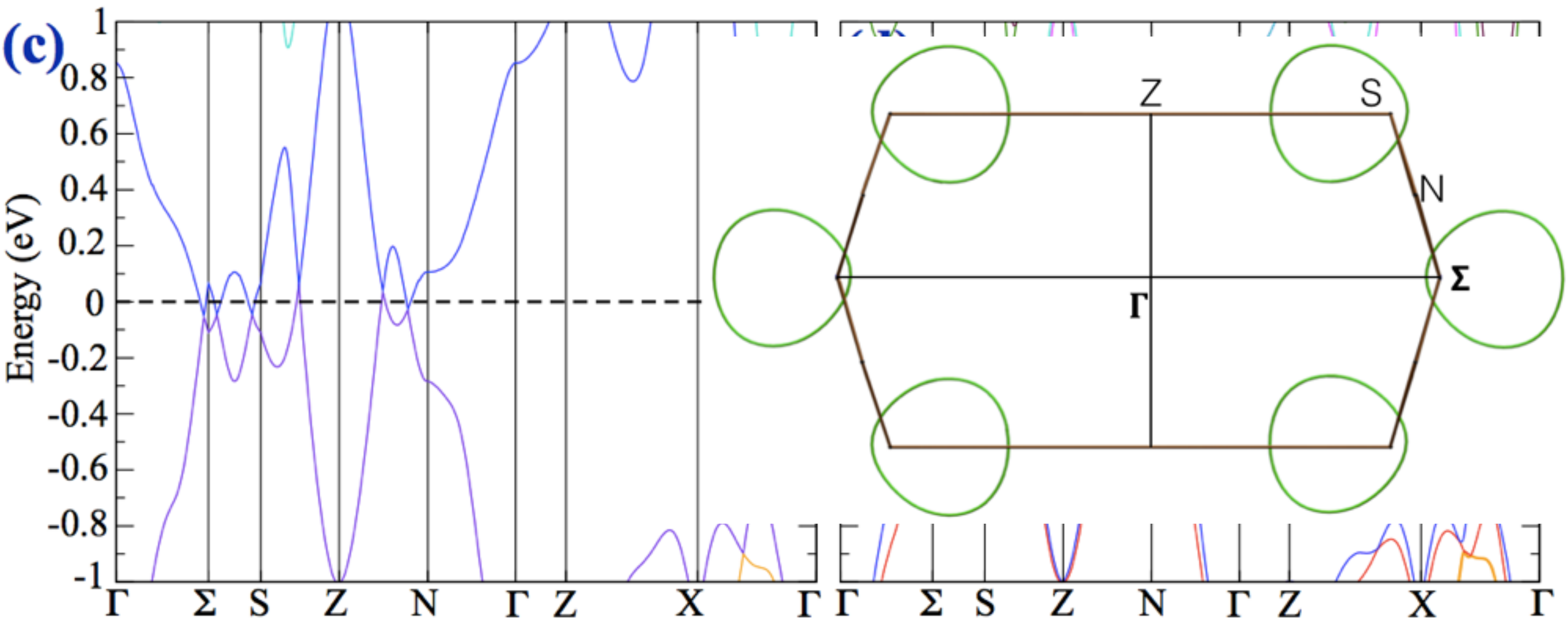

without SOC

Topological Node-Line Semimetal
http://arxiv.org/abs/1411.2175

3D View

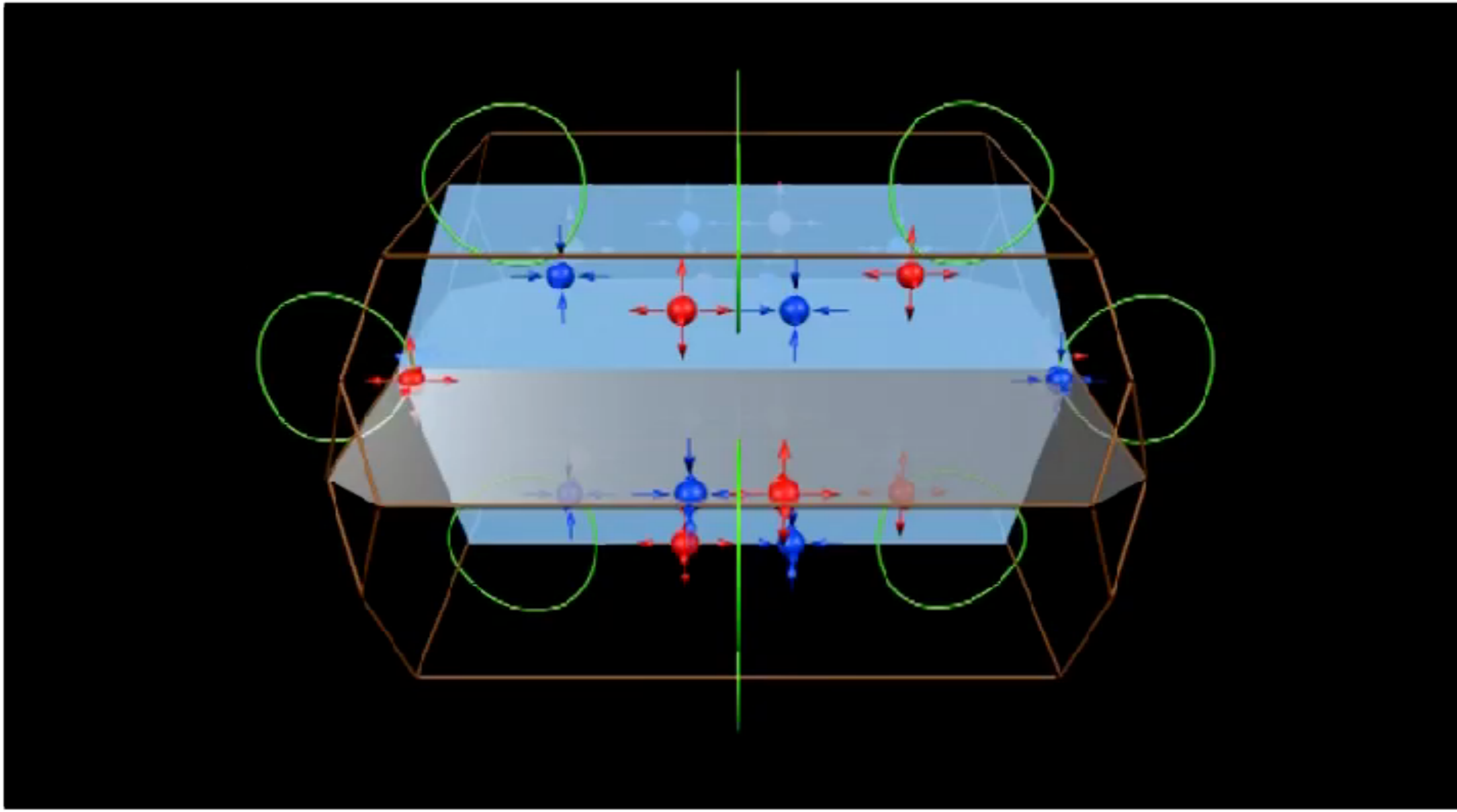

Surface Fermi arcs

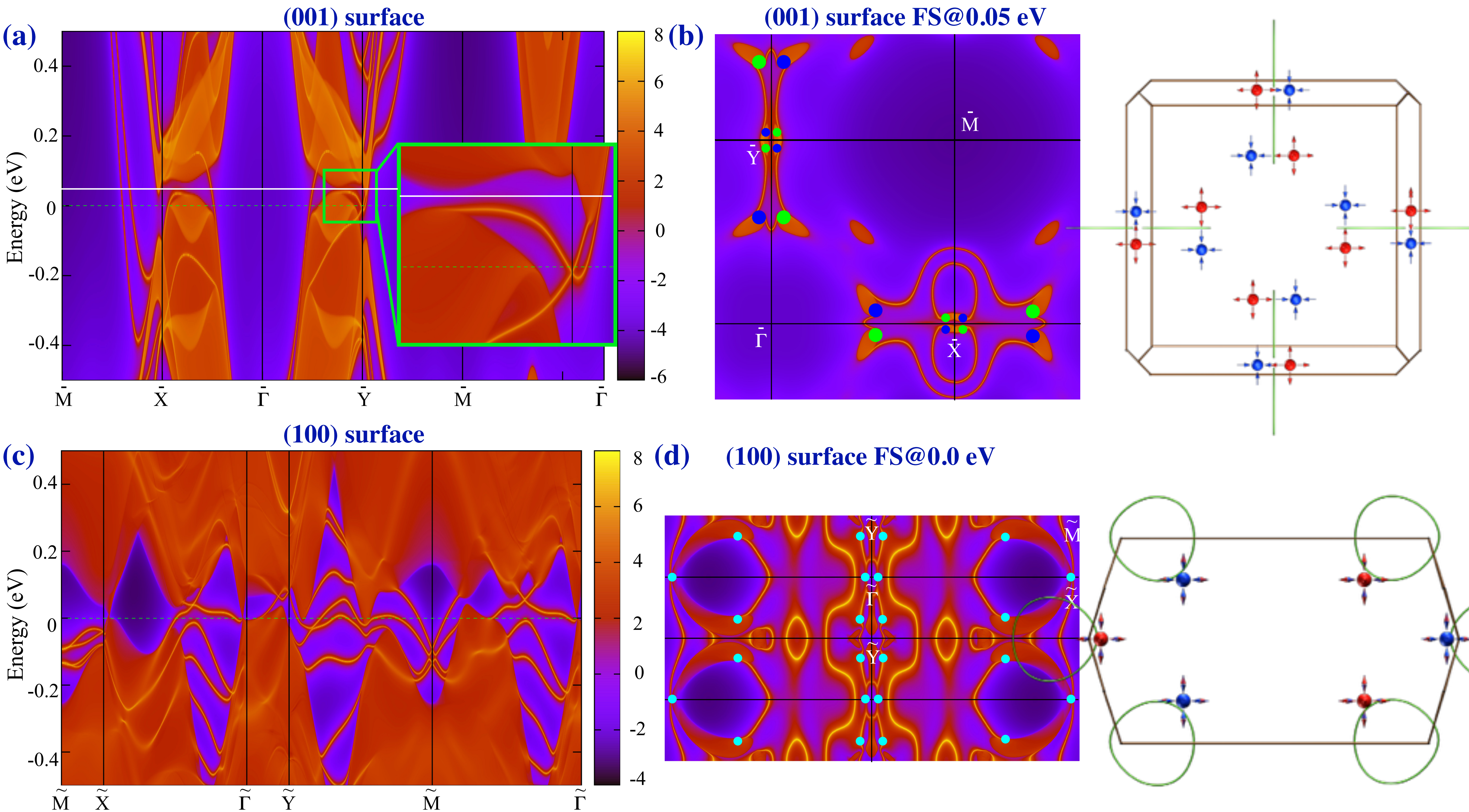

Experimental verification

up to early of Apr. 2015 from arXiv.

1	2015arXiv:1502.00251	Tantalum Monoarsenide: an Exotic Compensated Semimetal
2	2015arXiv:1502.03807	Experimental realization of a topological Weyl semimetal phase with Fermi arc surface states in TaAs @Science on Jul. 16, 2015 from Princeton & Peking University
3	2015arXiv:1502.04361	Extremely large magnetoresistance and ultrahigh mobility in the topological Weyl semimetal NbP
4	**2015arXiv:1502.04684**	**Discovery of Weyl semimetal TaAs** **@PRX on Jul. 16 from IOP, CAS**
5	**2015arXiv:1503.01304**	**Observation of the chiral anomaly induced negative magneto-resistance in 3D Weyl semi-metal TaAs** **@PRX on Jul. 20 from IOP, CAS**
6	2015arXiv:1503.02630	Observation of the Adler-Bell-Jackiw chiral anomaly in a Weyl semimetal
7	2015arXiv:1503.07571	Magnetotransport of single crystalline NbAs
8	**2015arXiv:1503.09188**	**Observation of Weyl nodes in TaAs** **@Nat. Phys. on Aug. 17 from IOP, CAS**
9	2015arXiv1504.01350	Discovery of Weyl semimetal NbAs @Nat. Phys. on Aug. 17 from Princeton & Peking University

Four hallmarks of Weyl semimetal observed in TaAs

1. “Chiral anomaly”— negative magnetoresistance

   arXiv:1503.01304 **Observation of the chiral anomaly induced negative magneto-resistance in 3D Weyl semi-metal TaAs** IOP, CAS group

   arXiv:1503.02630 Observation of the Adler-Bell-Jackiw chiral anomaly in a Weyl semimetal PU&PKU group

2. Fermi arcs

   arXiv:1502.03807 Experimental realization of a topological Weyl semimetal phase with Fermi arc surface states in TaAs PU&PKU group

   arXiv:1502.04684 **Discovery of Weyl semimetal TaAs** IOP, CAS group

3. Bulk Weyl nodes

   arXiv:1502.03807 Experimental realization of a topological Weyl semimetal phase with Fermi arc surface states in TaAs PU&PKU group

   arXiv:1503.09188 **Observation of Weyl nodes in TaAs** IOP, CAS group

4. Spin texture of Fermi arc

   arXiv:1510.07256 **Observation of spin texture of Fermi arc of TaAs** IOP, CAS group

Breakthrough & Highlight of 2015

Weyl fermions are spotted at long last

To Zahid Hasan of Princeton University, Marin Soljačić of MIT, and Zhong Fang and Hongming Weng of the Chinese Academy of Sciences, for their pioneering work on Weyl fermions. These massless particles were predicted by the German mathematician Hermann Weyl in 1929. Working independently, a team led by Hasan, and another led by Fang and Weng, spotted telltale evidence

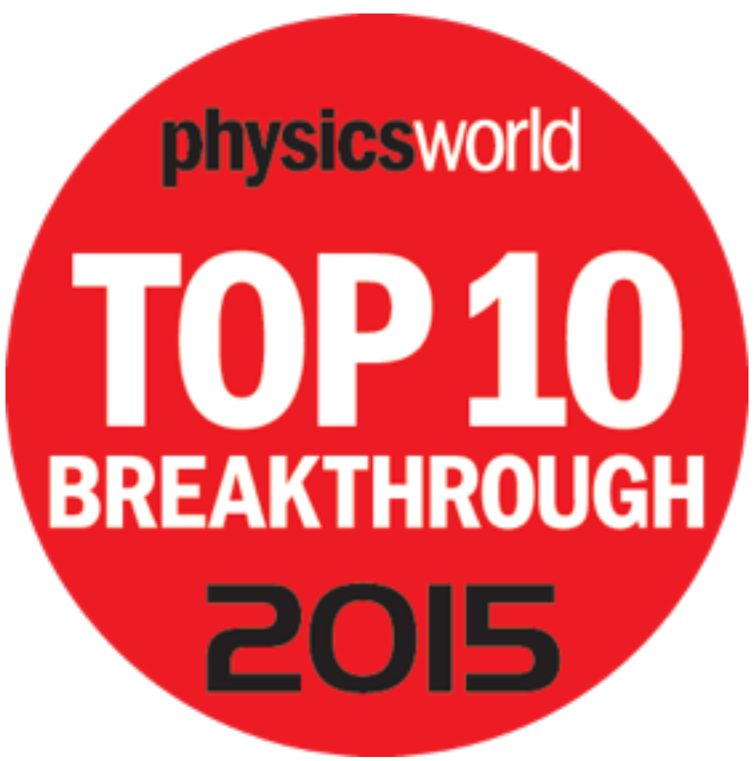

IOP

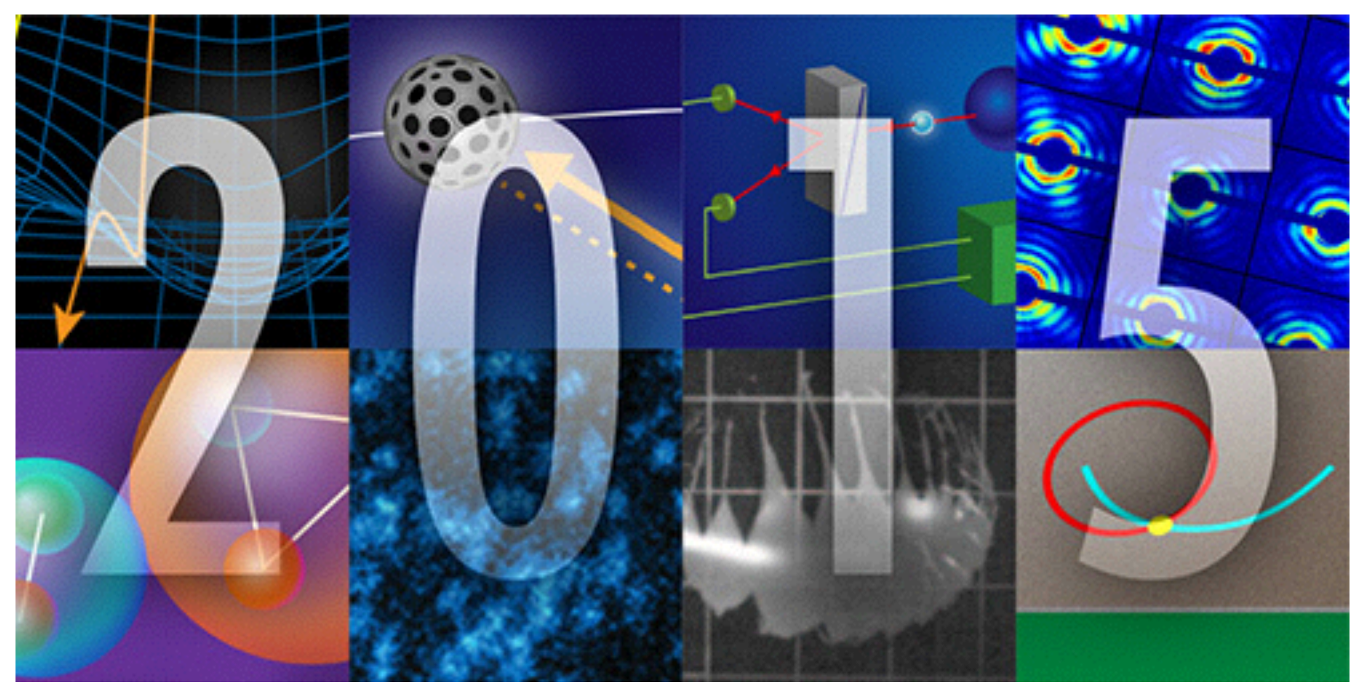

APS

Triply Degenerate Nodal Point

A New Massless Fermion

Weng, Fang, et al., PRB **93**, 241202(R) (2016)

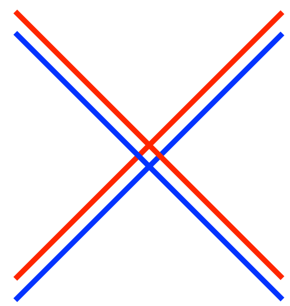

DSM

(4x4)

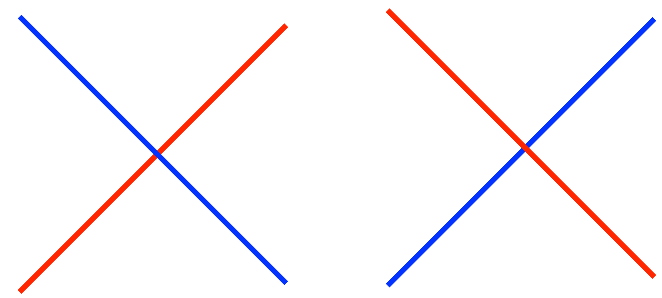

WSM

(2x2)

		E	C2	2C3	2C6	3IC2`	3IC2"
G1	A1	1	1	1	1	1	1
G2	A2	1	1	1	1	−1	−1
G3	B1	1	−1	1	−1	1	−1
G4	B2	1	−1	1	−1	−1	1
G5	E1	2	−2	−1	1	0	0
G6	E2	2	2	−1	−1	0	0
G7	E1/2	2	0	1	/3	0	0
G8	E5/2	2	0	1	−/3	0	0
G9	E3/2	2	0	−2	0	0	0

Na_3Bi Γ-A C6v

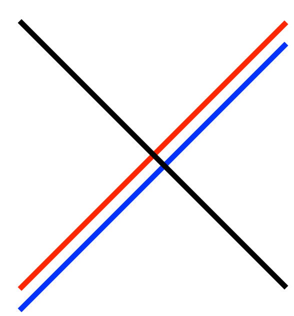

TDNP

(3x3)

Point group C3v

		E	2C3	3IC2
G1	A1	1	1	1
G2	A2	1	1	-1
G3	E	2	-1	0
G4	E1/2	2	1	0
G5	1E3/2	1	-1	i
G6	2E3/2	1	-1	-i

Triply Degenerate Nodal Point

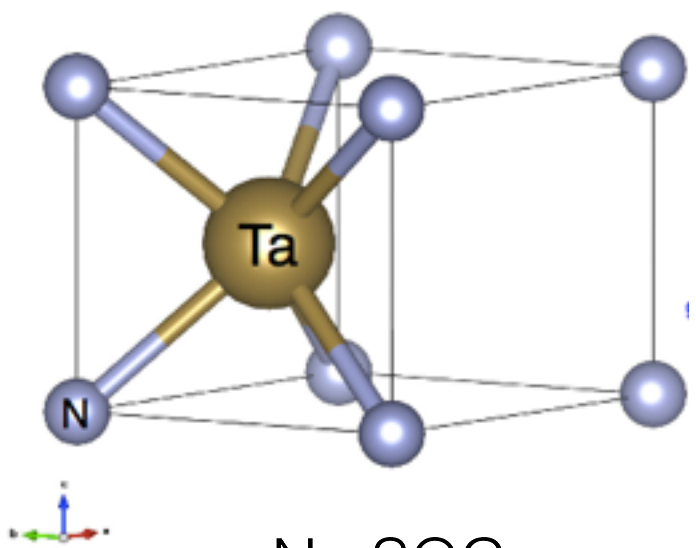

WC-type
TaN, NbN, ZrTe *etc.*

No SOC

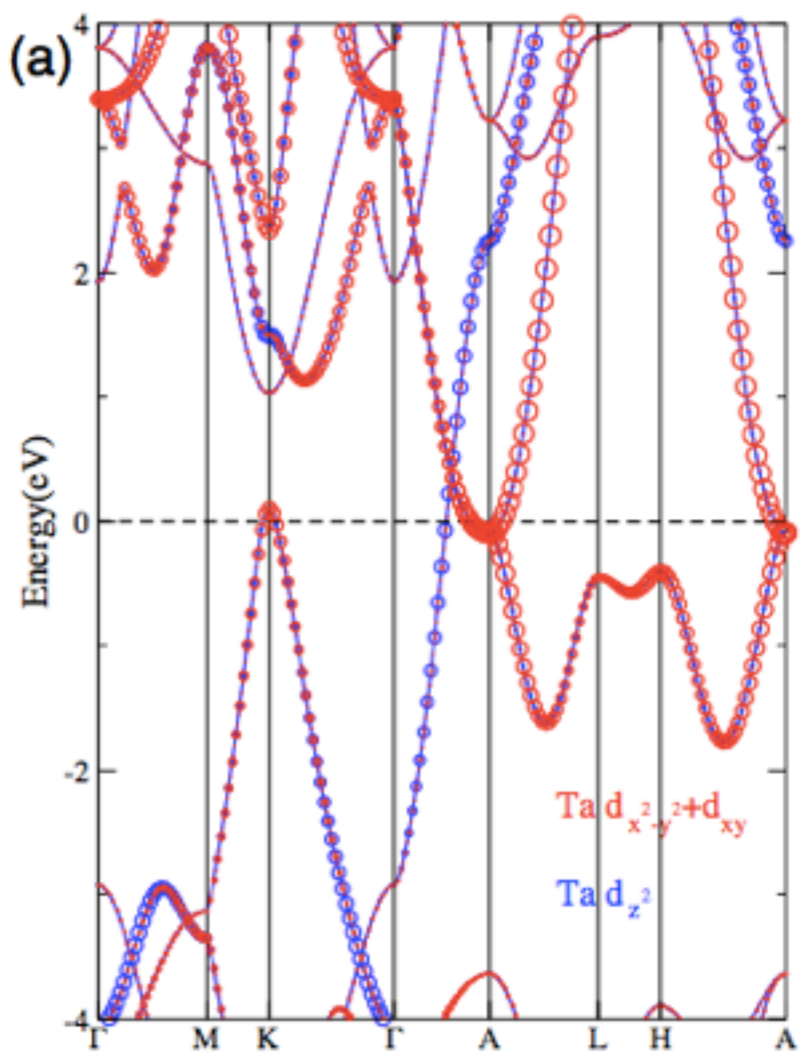

+SOC

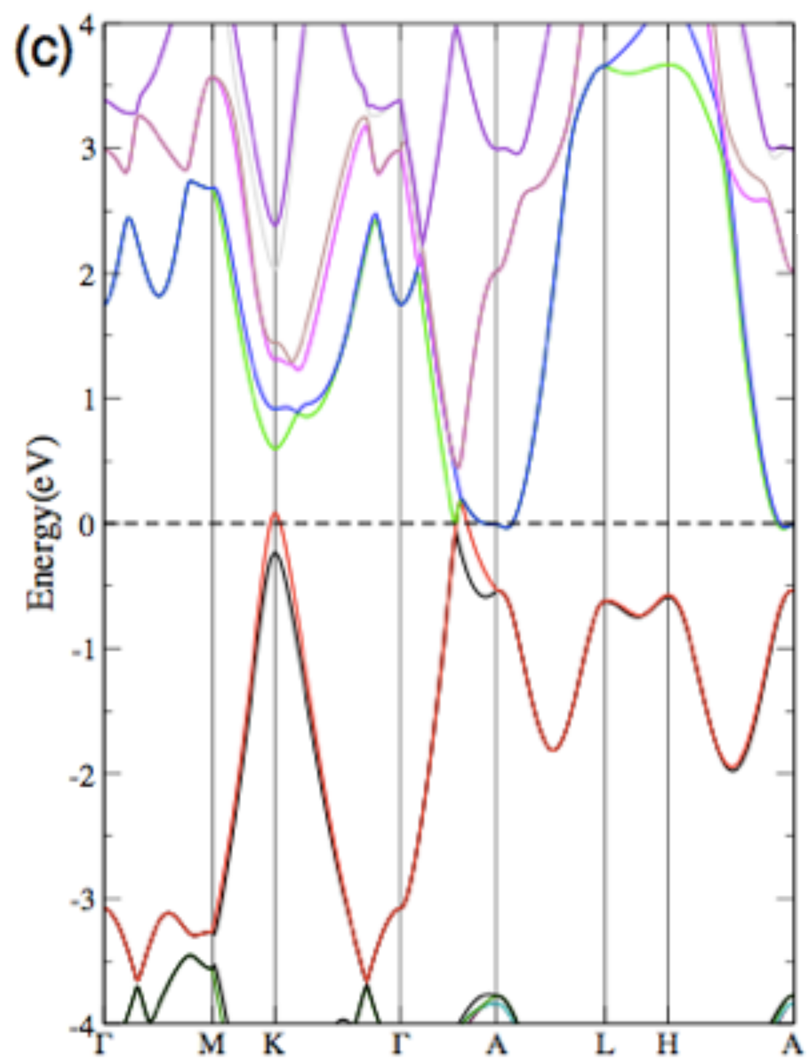

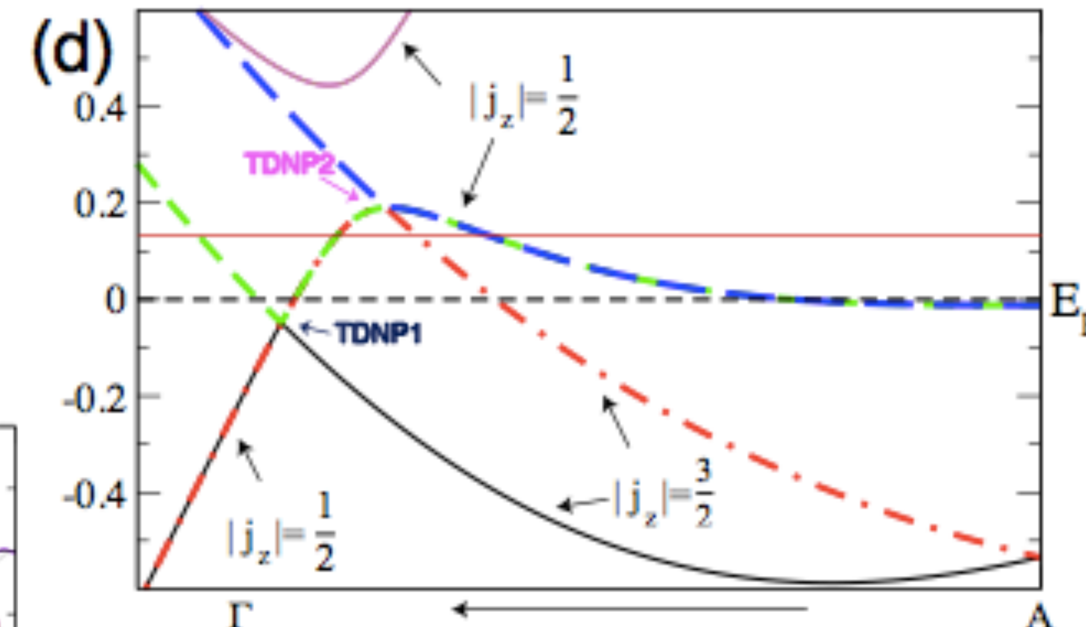

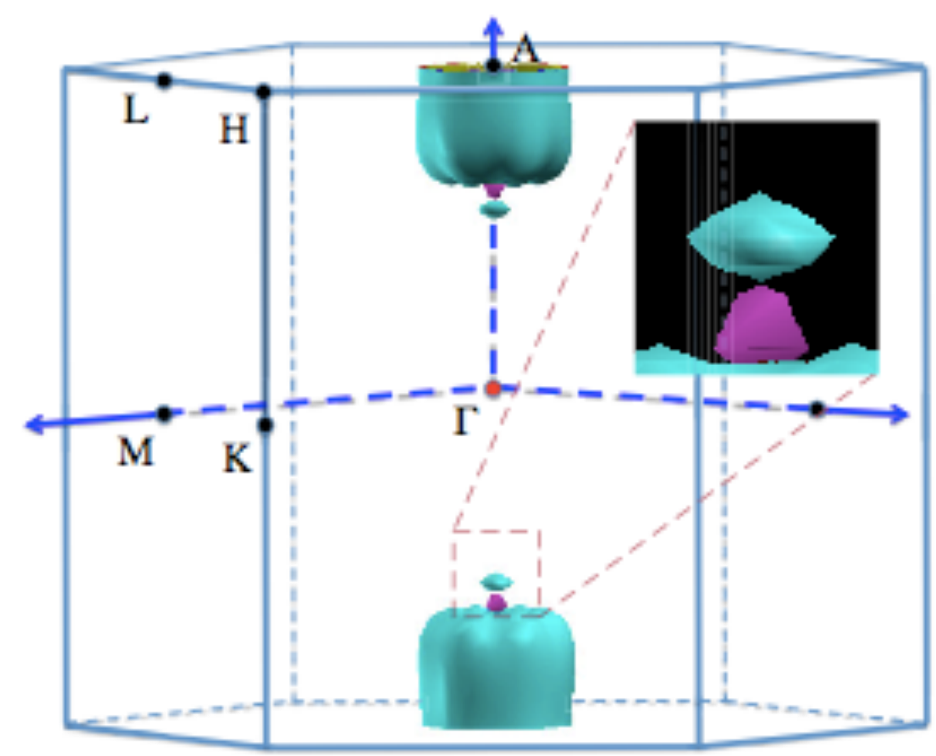

Triply Degenerate Nodal Point

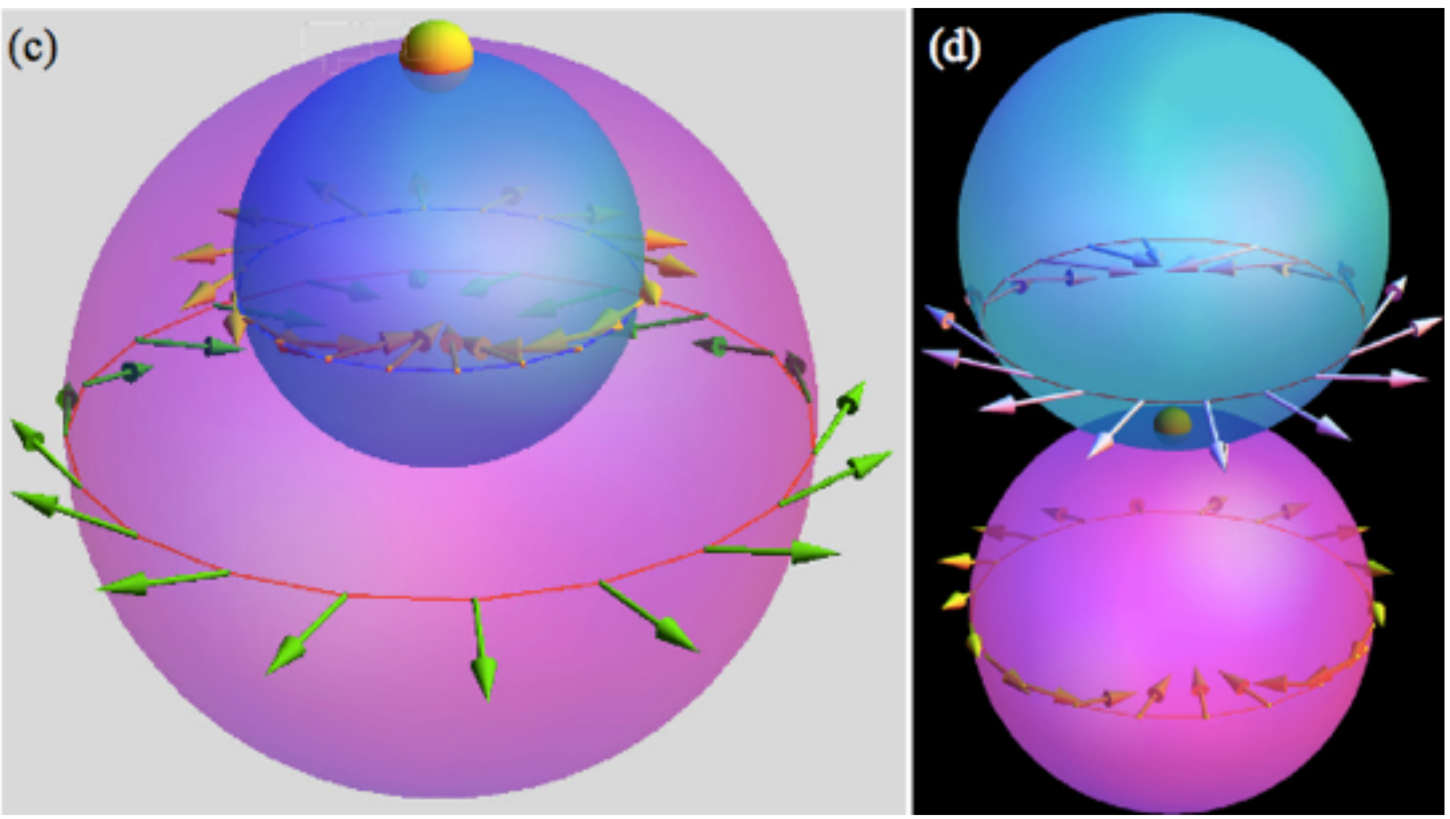

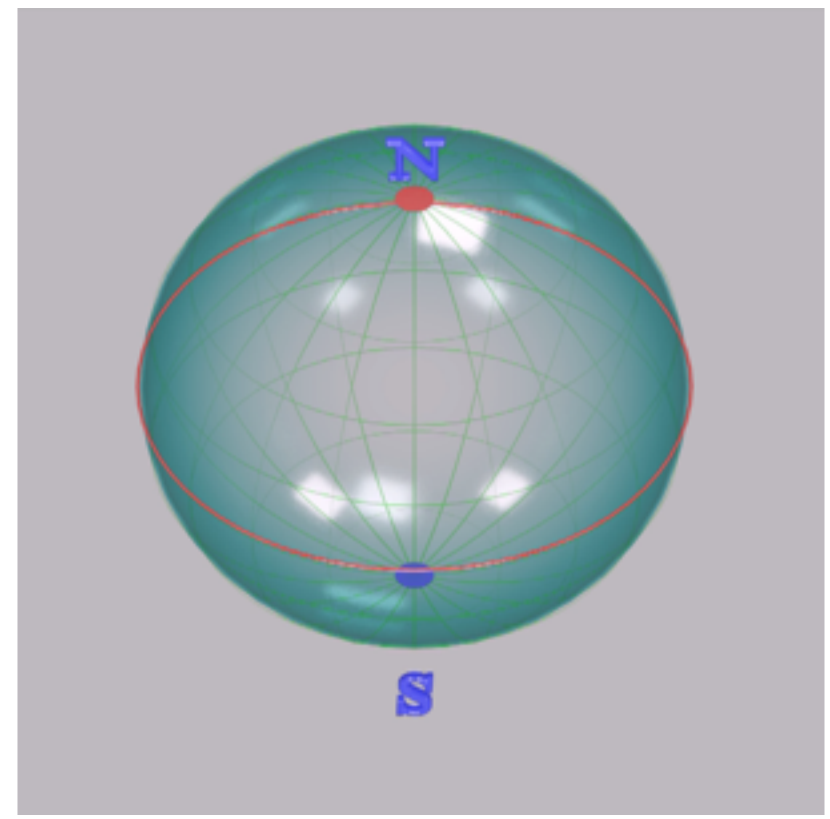

Winding number 2 for spin on the Fermi surface

Triply Degenerate Nodal Point

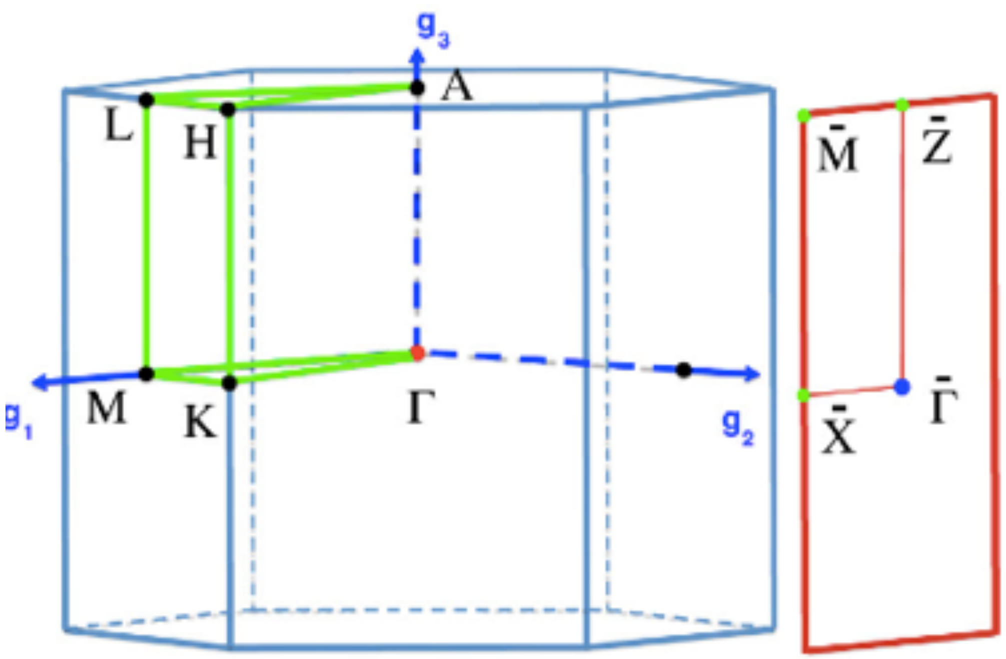

(100) surface

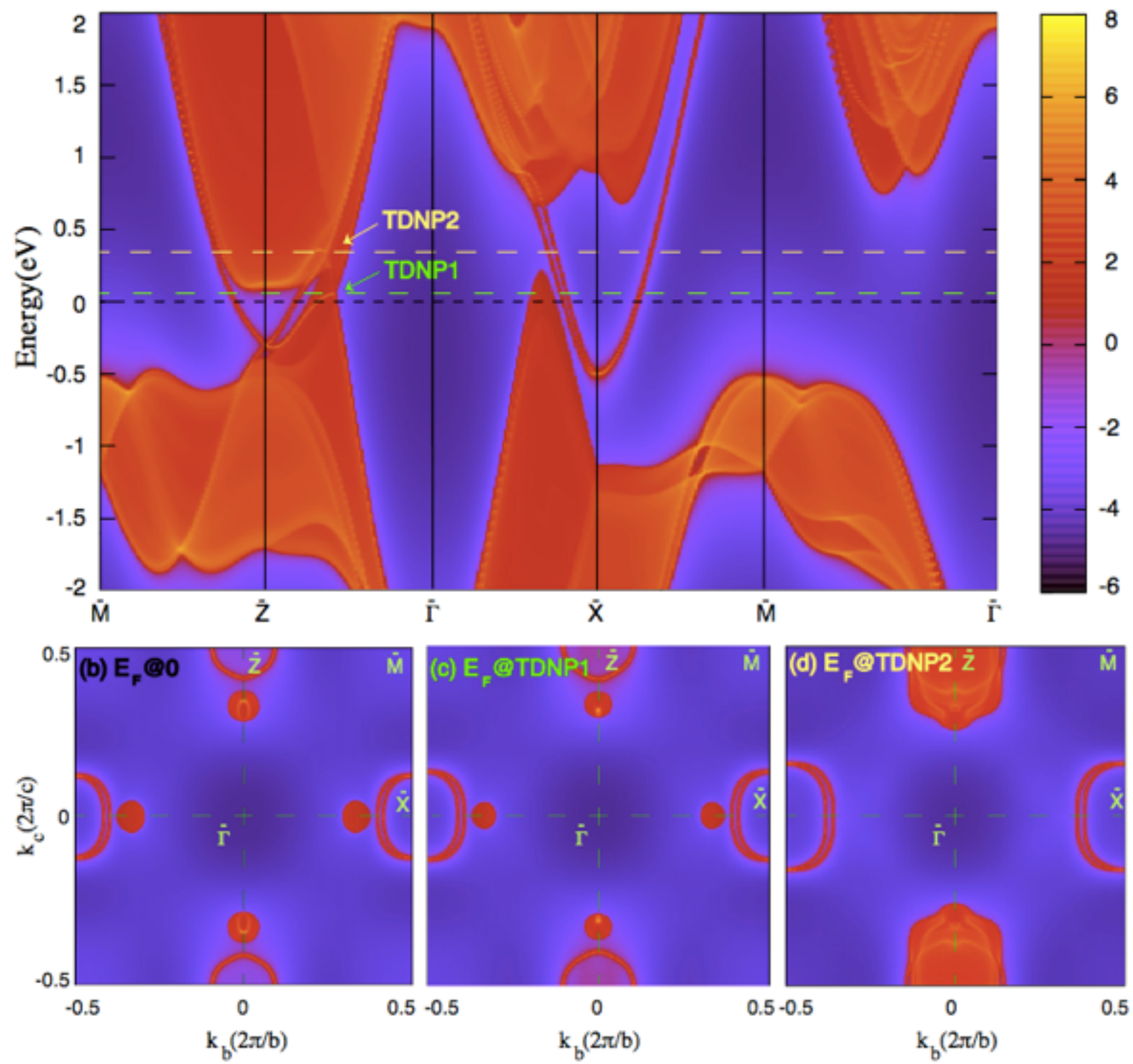

Triply Degenerate Nodal Point

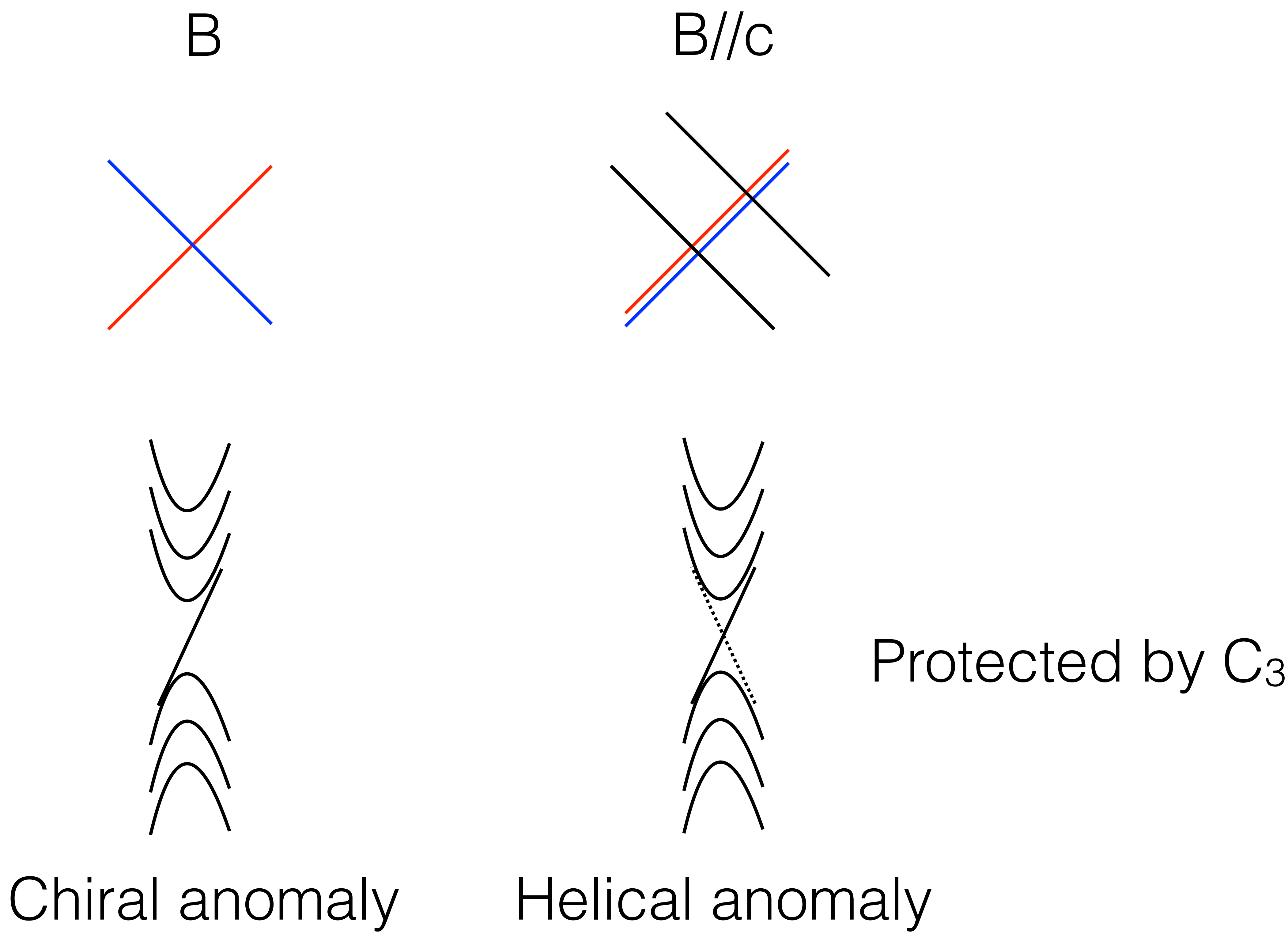

Weyl nodal points Co-exist with Triply Degenerate Nodal Points

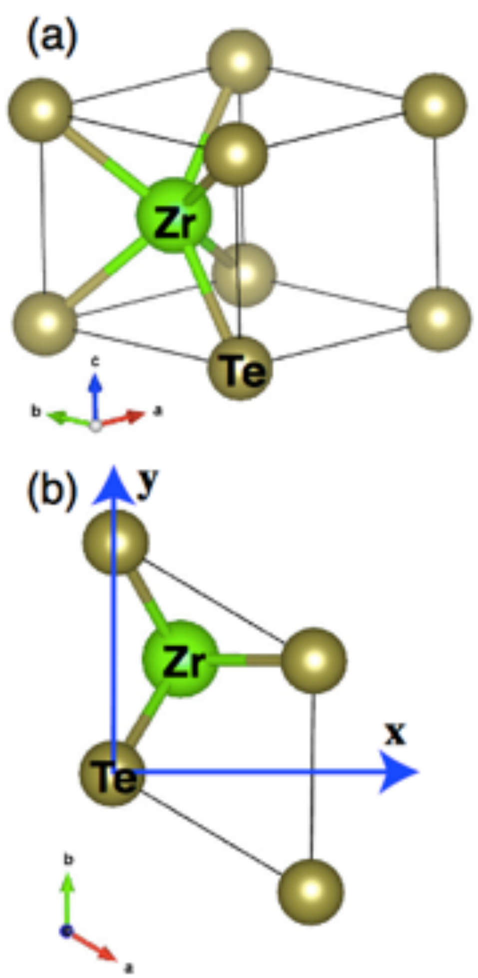

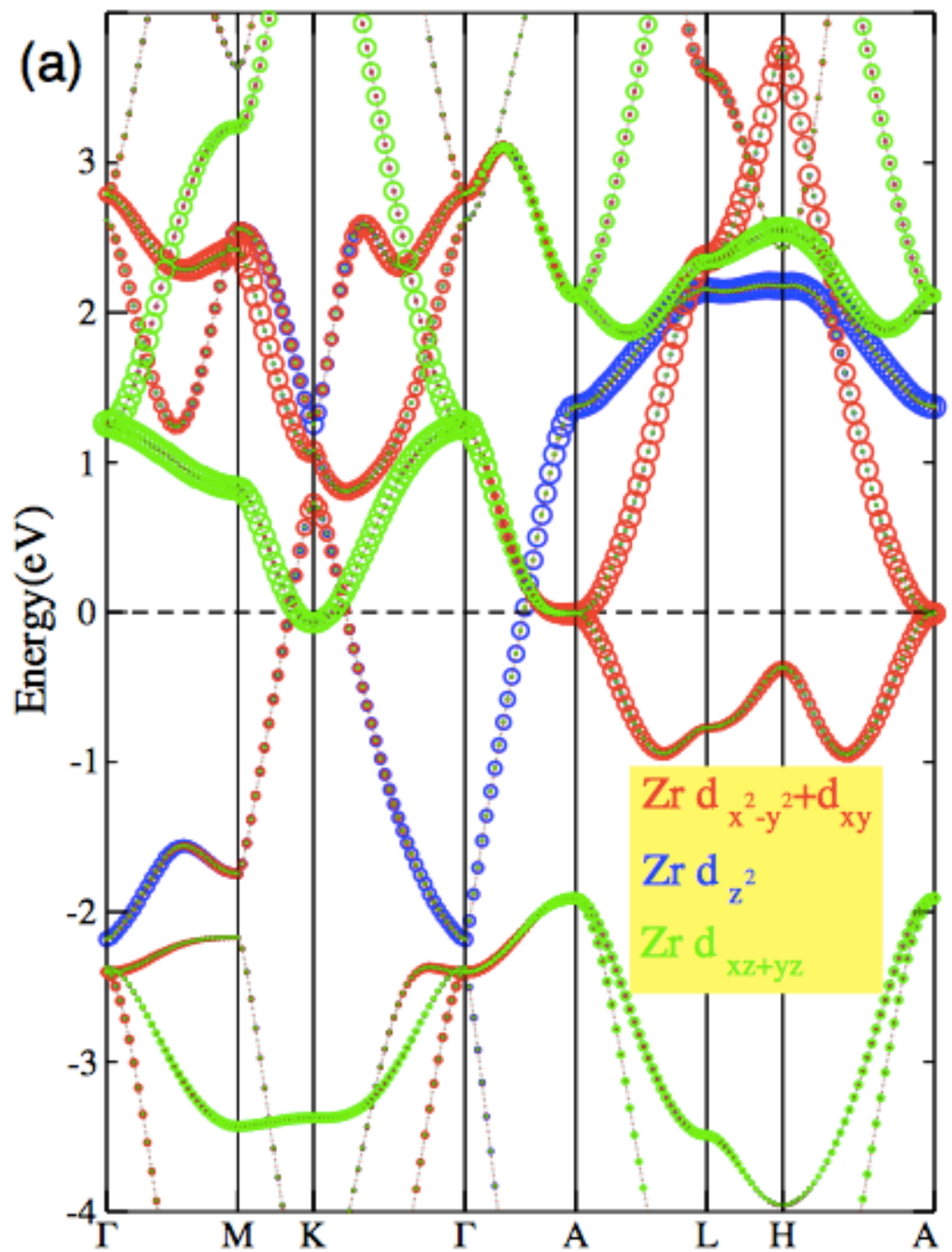

Weng, Fang, et al. arXiv:1605.05186

Weyl points co-exist with Triply Degenerate Nodal Points

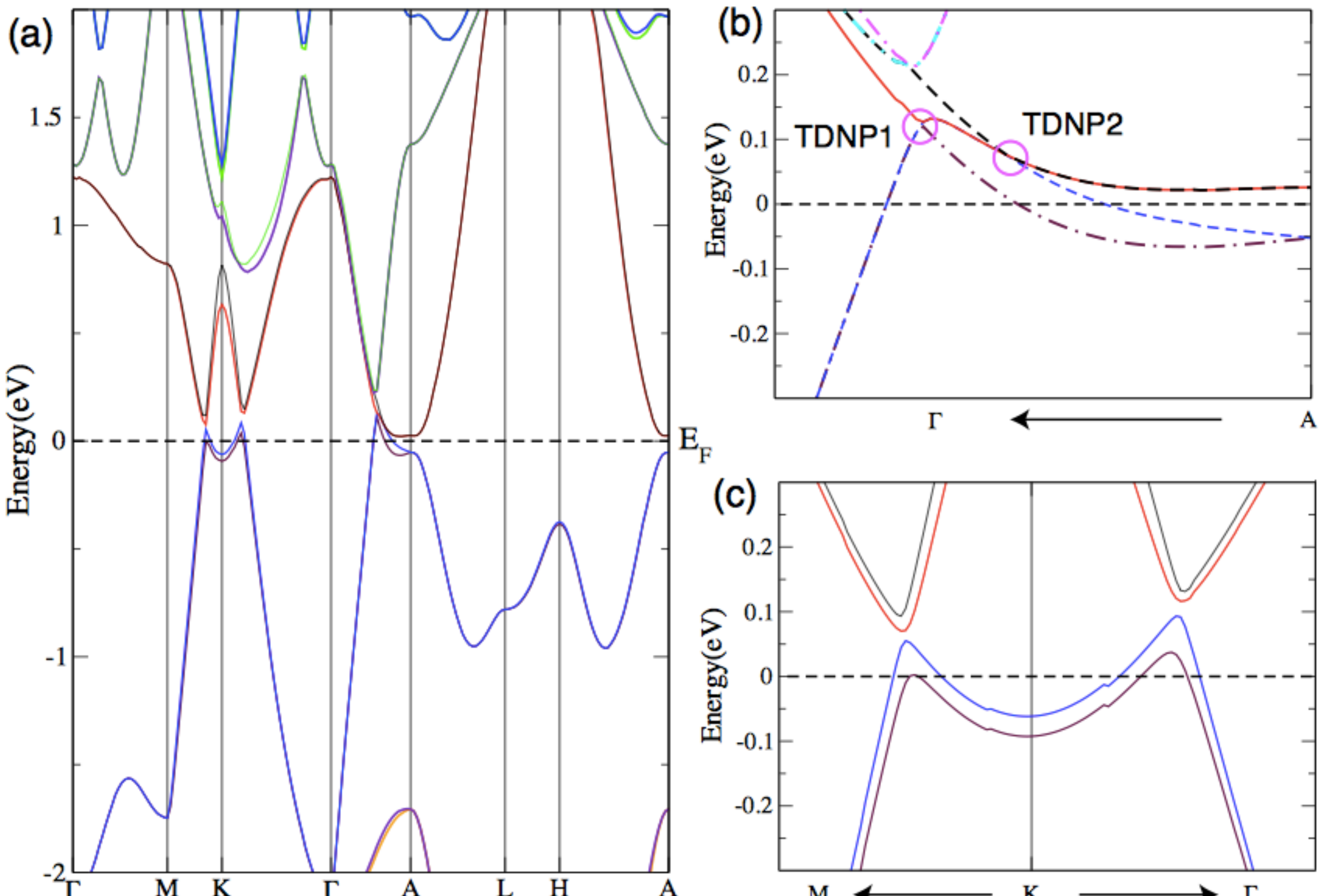

Weng, Fang, et al. arXiv:1605.05186

Weyl points co-exist with Triply Degenerate Nodal Points

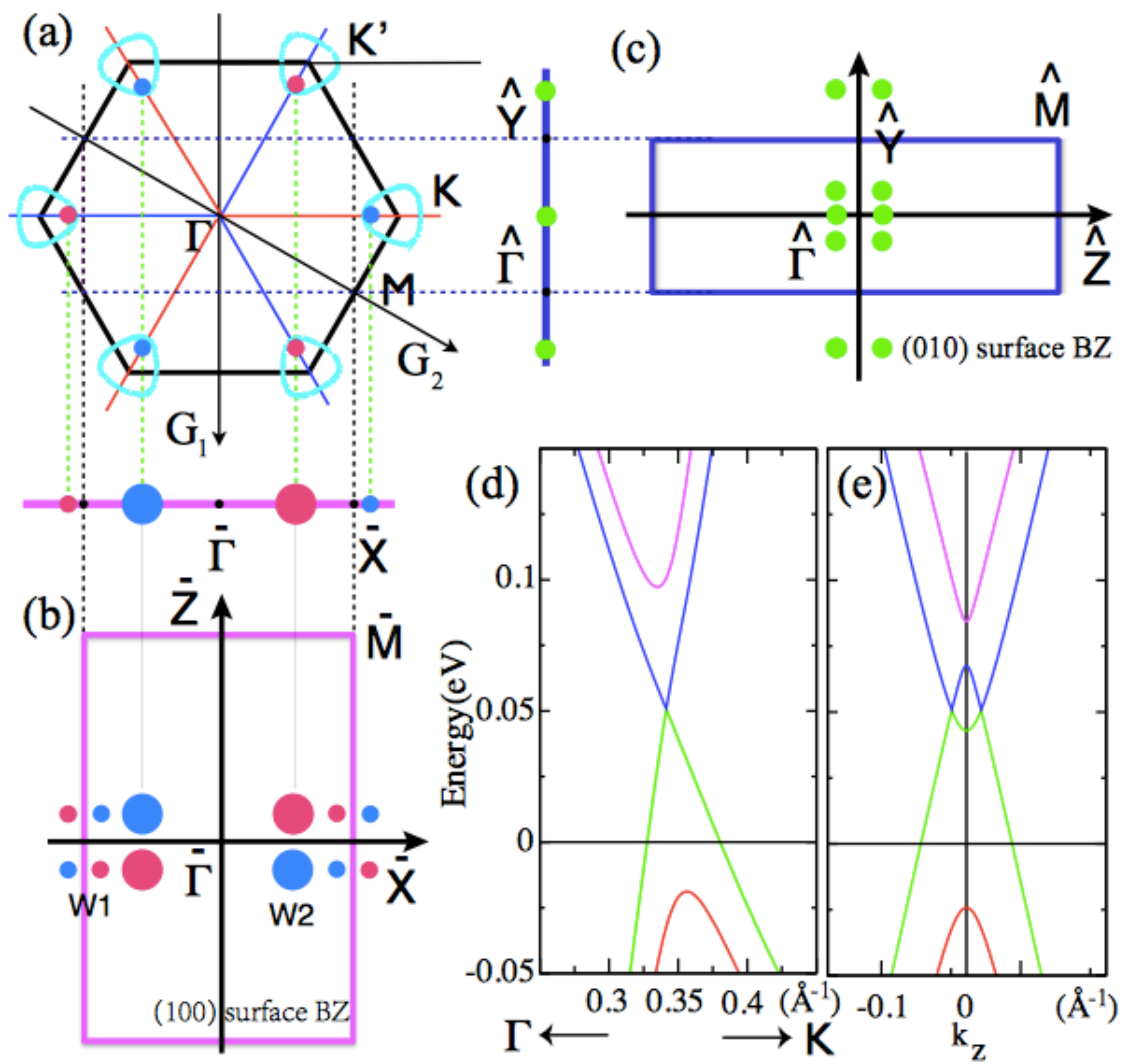

@50meV

Weng, Fang, et al. arXiv:1605.05186

Weyl points co-exist with Triply Degenerate Nodal Points

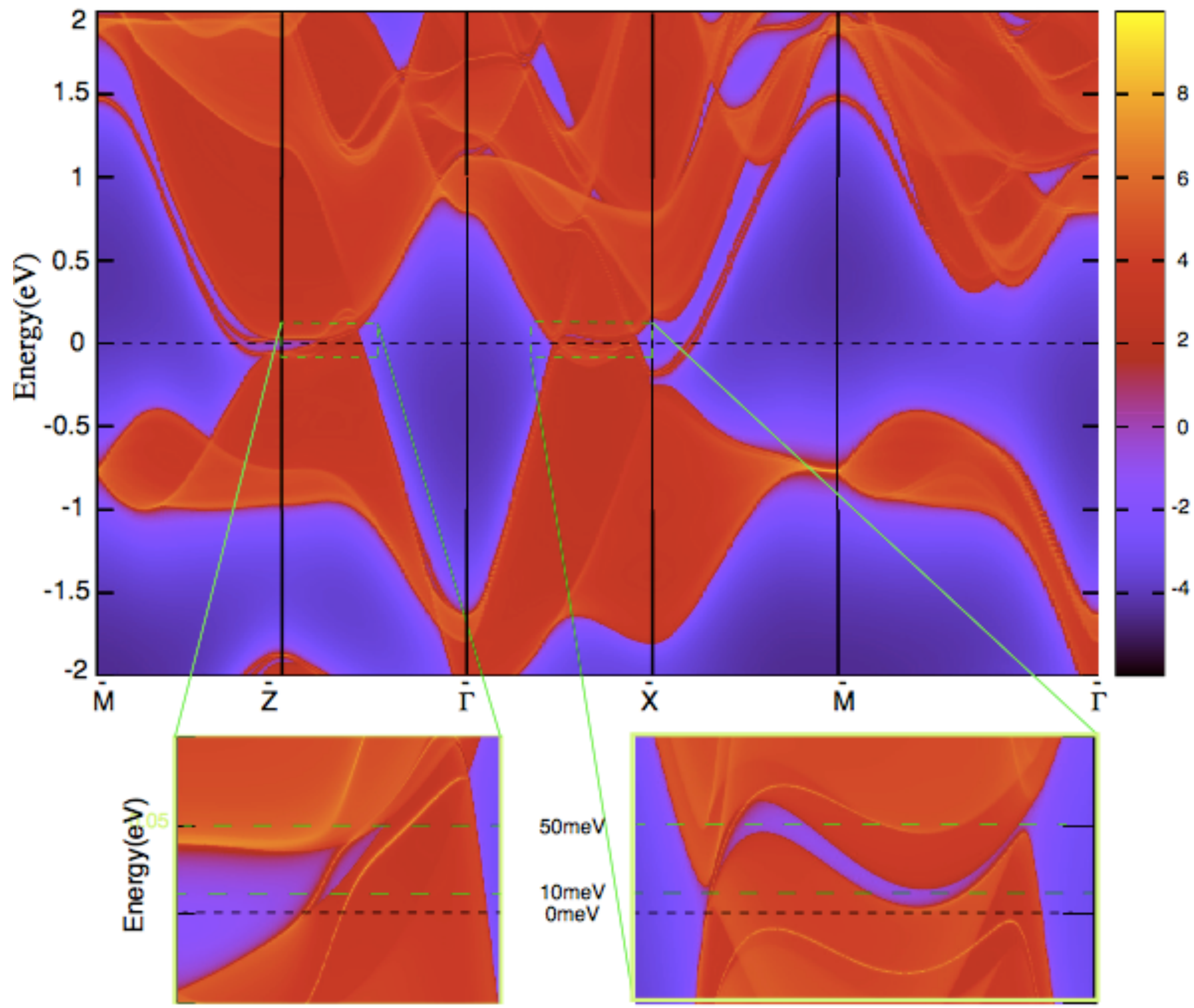

(Color online) ZrTe (100) surface state with its band structure weighted

Weng, Fang, et al. arXiv:1605.05186

Weyl points co-exist with Triply Degenerate Nodal Points

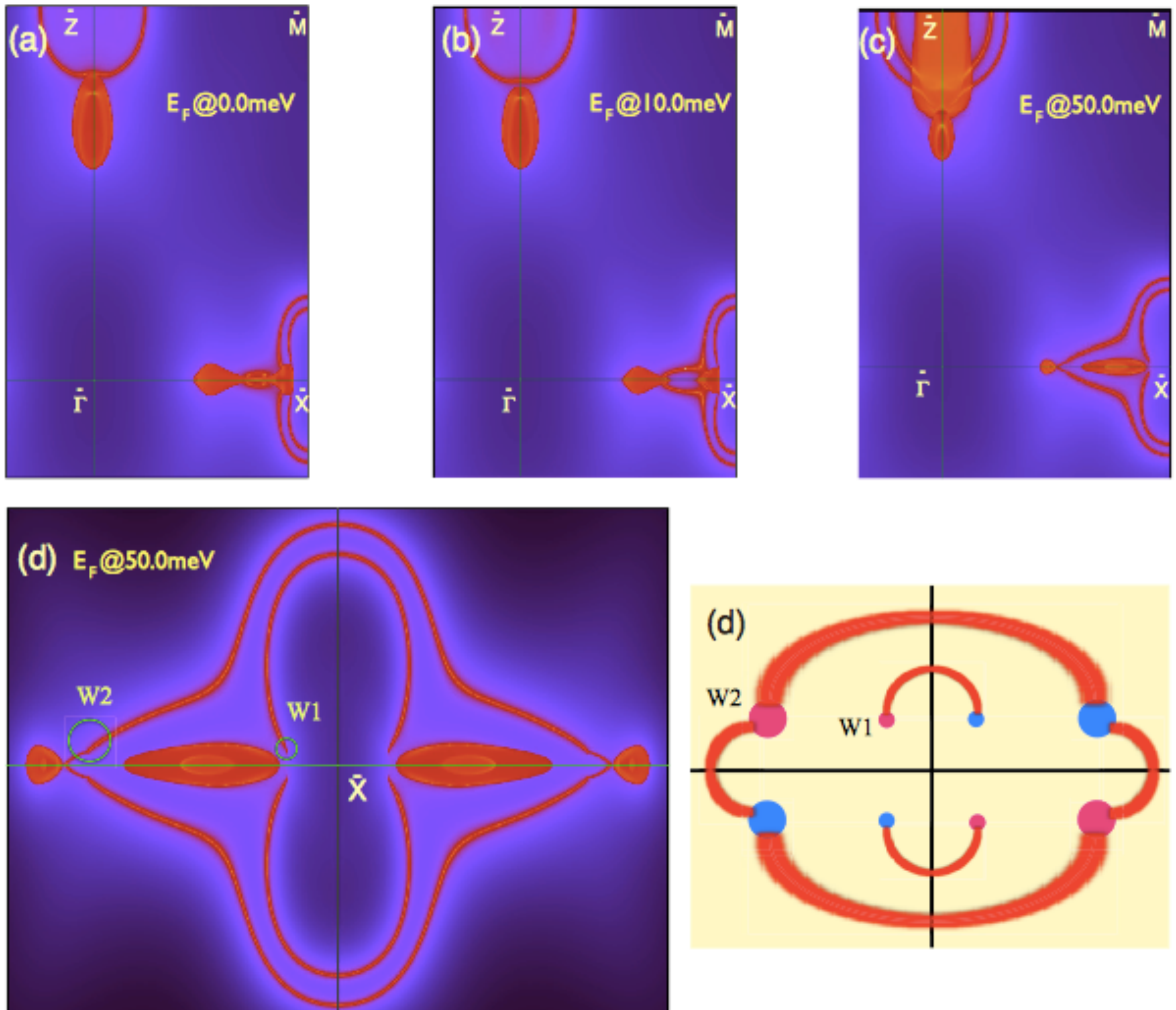

(100) surface

Weng, Fang, et al. arXiv:1605.05186

Weyl points co-exist with Triply Degenerate Nodal Points

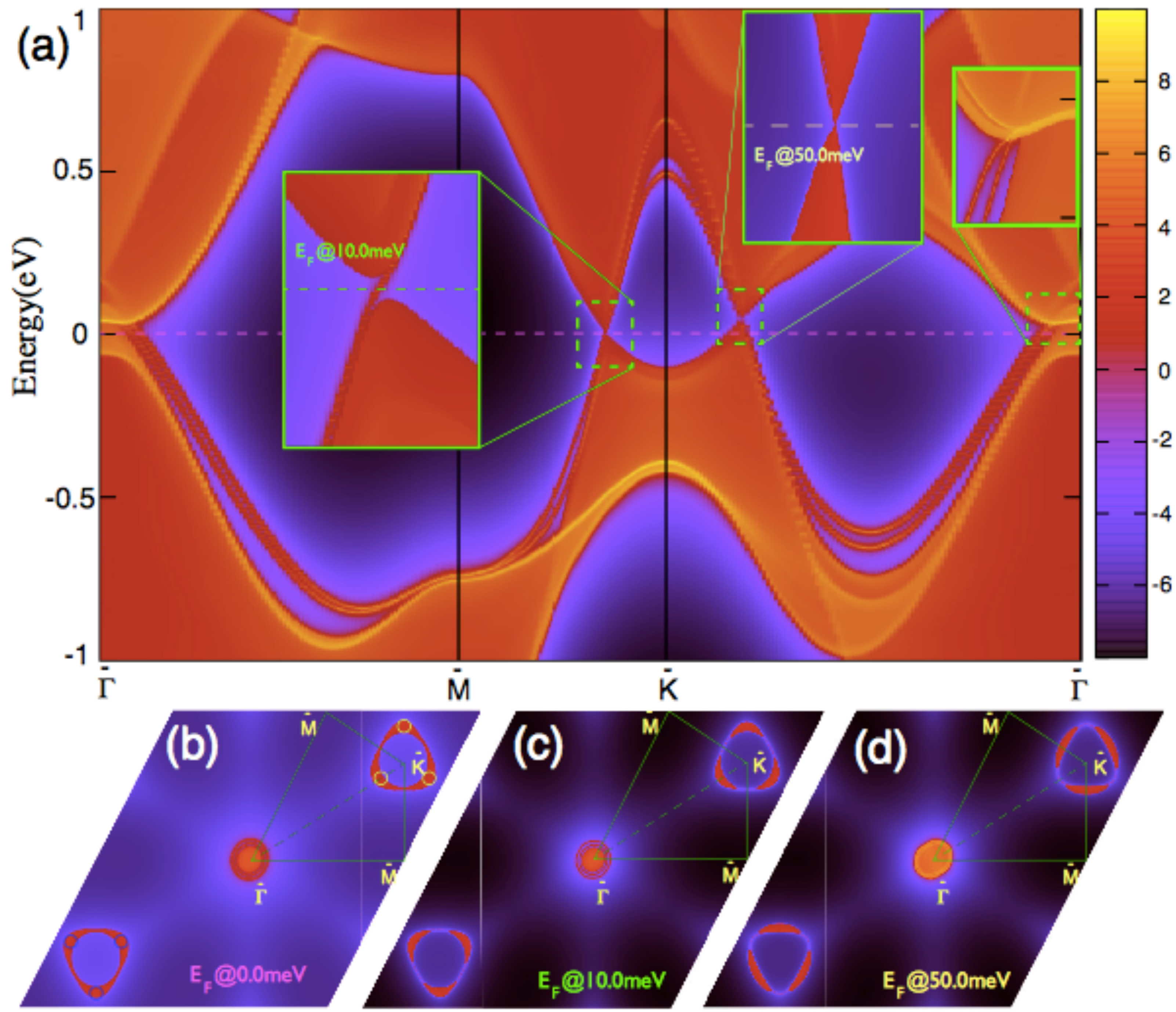

Weng, Fang, et al. arXiv:1605.05186

Weyl points co-exist with Triply Degenerate Nodal Points

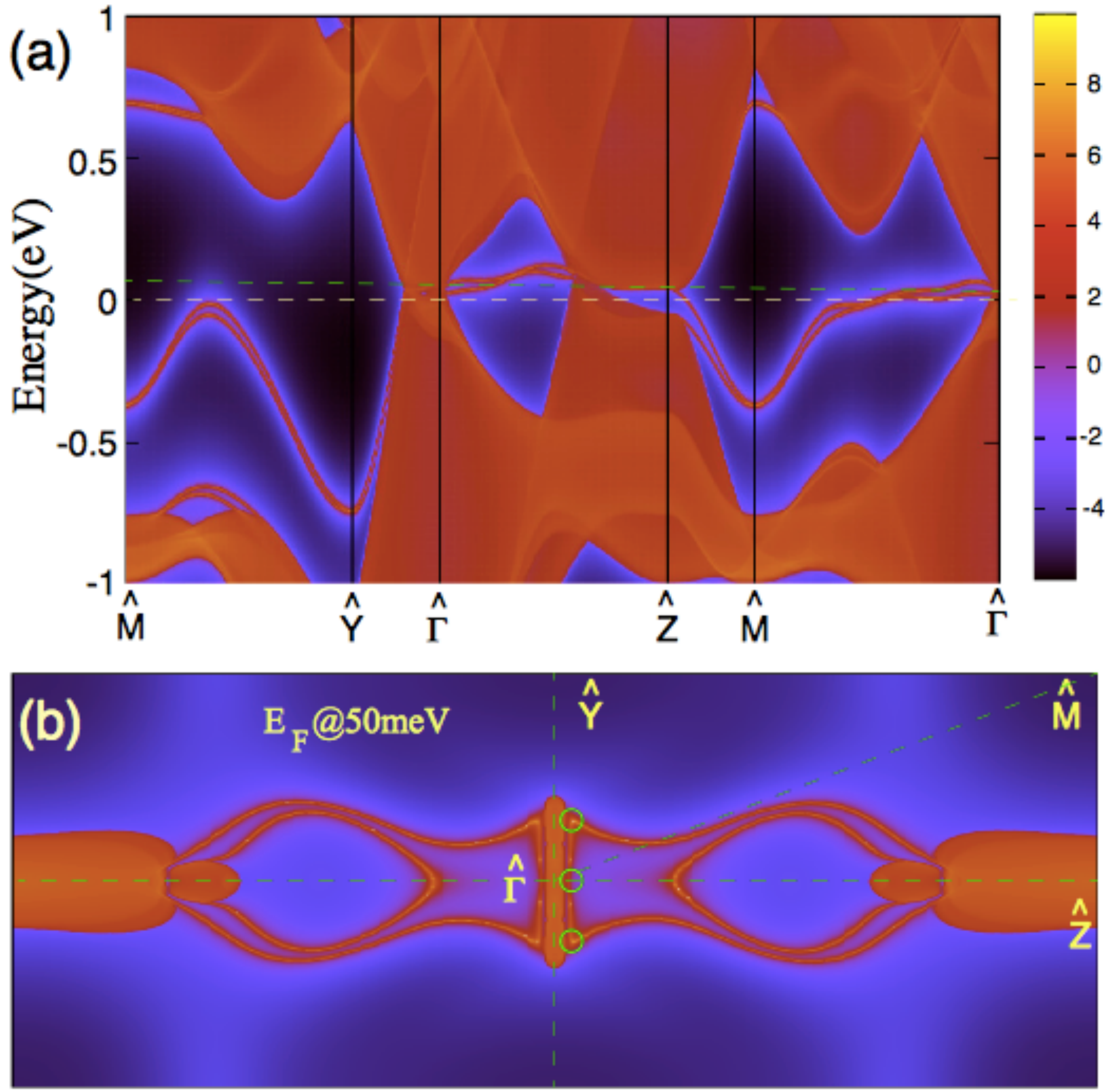

Weng, Fang, et al. arXiv:1605.05186

Topological Semimetal Family

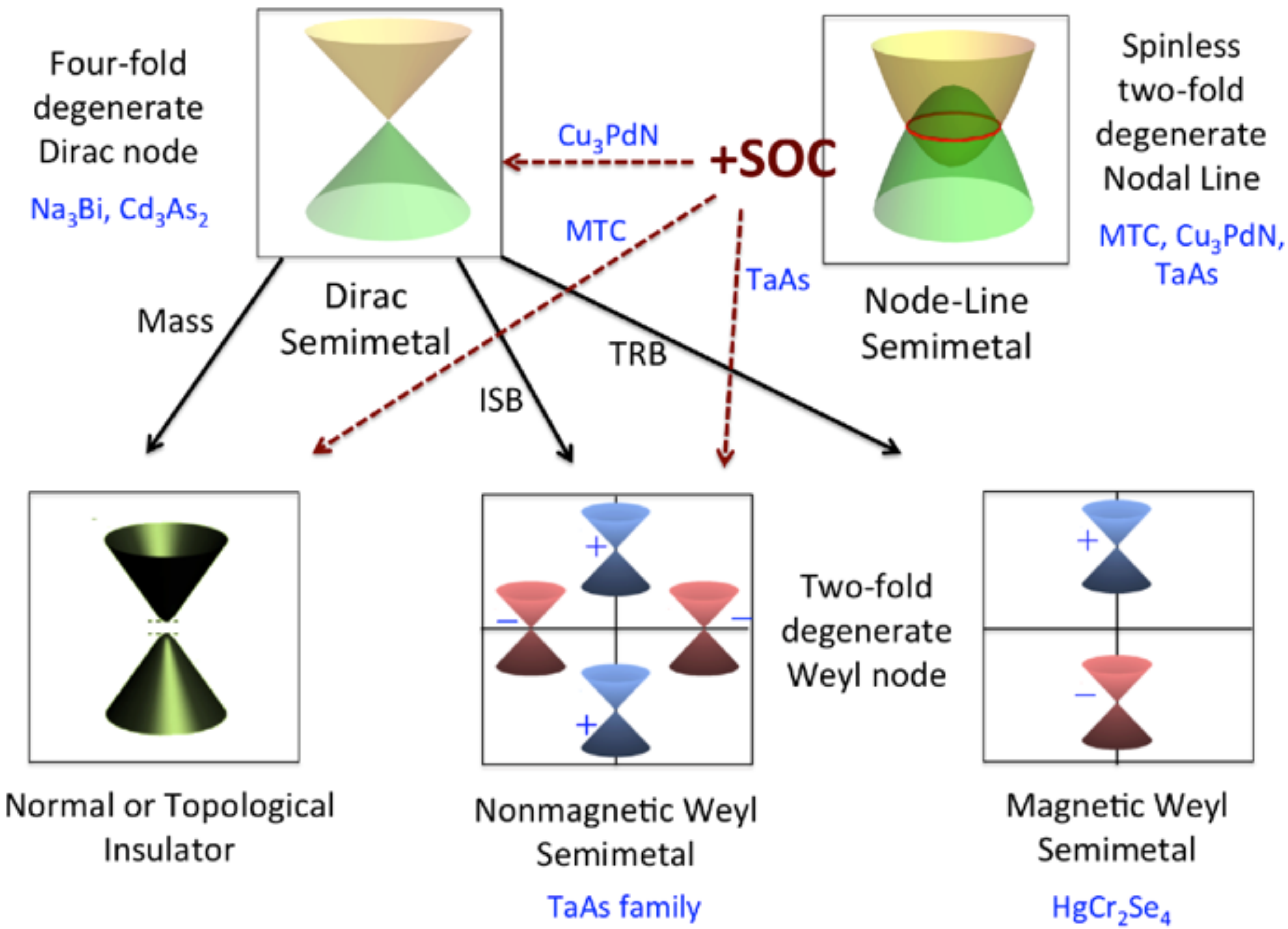

a New member

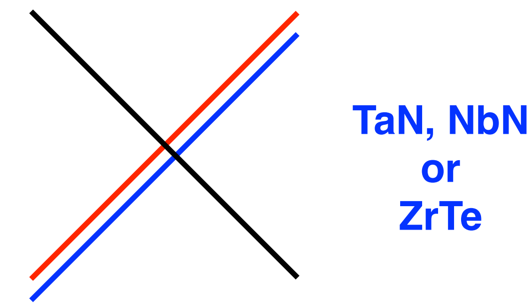

TDNP

arXiv:1604.08467,
arXiv:1605.05186

a review: H. Weng, X. Dai and Z. Fang, J. Phys.:Condens. Matter 28, 303001 (2016)

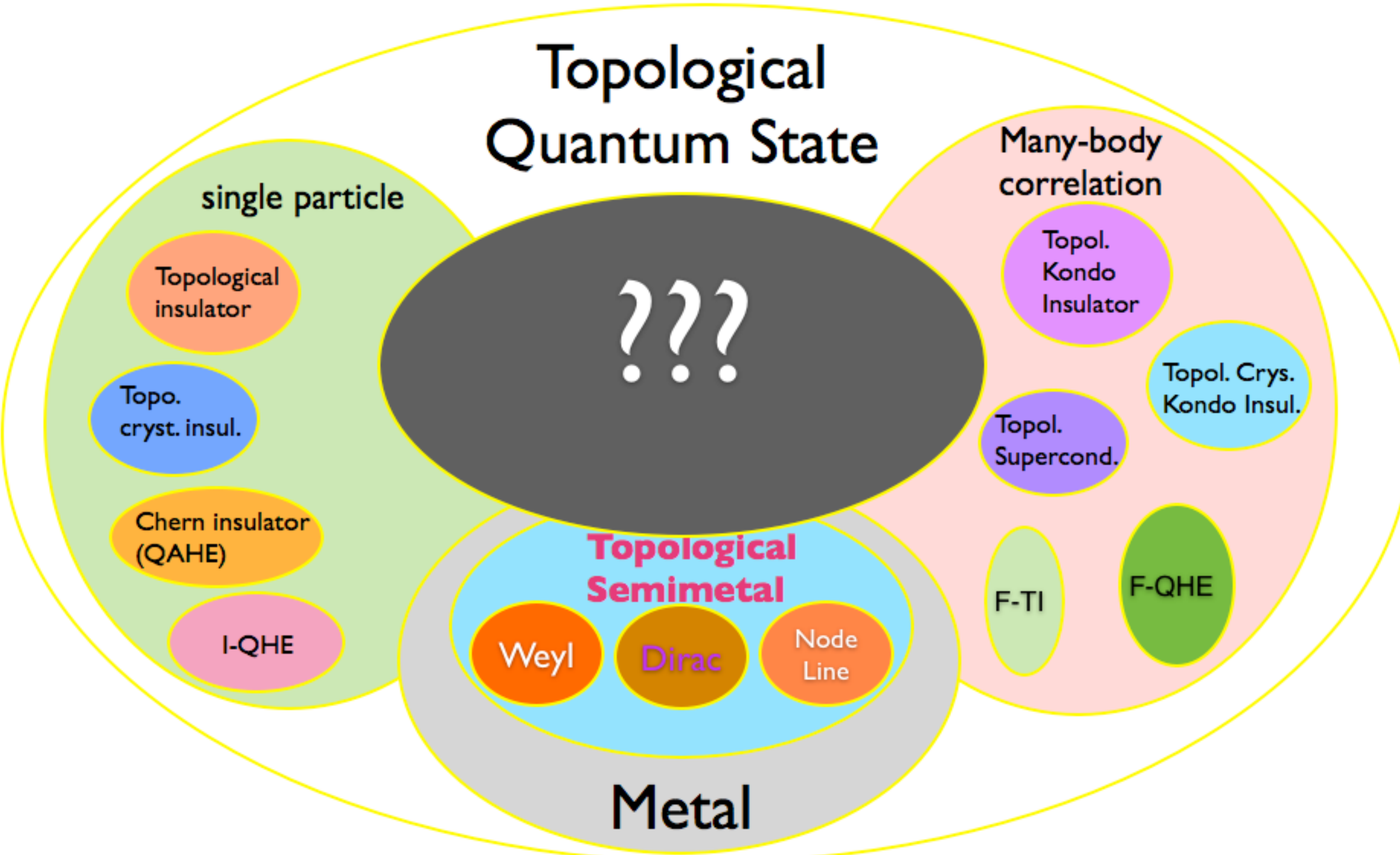

Thank you for your attention !